ISSN Application No. 21807

Journal of Industrial and Mechanical Engineering

Volume No. 7

Issue No. 2

May - August 2023

ENRICHED PUBLICATIONS PVT. LTD

S-9, IInd FLOOR, MLU POCKET,
MANISH ABHINAV PLAZA-II, ABOVE FEDERAL BANK,
PLOT NO-5, SECTOR-5, DWARKA, NEW DELHI, INDIA-110075,
PHONE: - + (91)-(11)-47026006

Journal of Industrial and Mechanical Egineering

Aims and Scope

Journal of Industrial and Mechanical Engineering is a peer-reviewed journal for the presentation of original contributions and the exchange of knowledge and experience on mechanical and industrial engineering topics like Acoustics and Noise Control, Aerodynamics, Agricultural machinery, Applied Mechanics, Automation, Mechatronics and Robotics, Automobiles, Automotive Engineering, Ballistics, Biomechanics, Biomedical Engineering, Composite and Smart Materials, Composite Materials, Compressible Flows, Computational Mechanics, Computational Techniques, Dynamical Analyses, Dynamics and Vibration, Energy Engineering and Management, Engineering Materials, Fatigue and Fracture, Fluid Dynamics, Fluid Mechanics and Machinery etc.

Journal of Industrial and Mechanical Engineering

Journal of Industrial and Mechanical Engineering

(Volume No. 7, Issue No. 2, May - August 2023)

Contents

A Two-Stage Heuristic for Dispatching Capacitated Multi-Vehicle Routing with Time Window Constraints

Saleem Z Ramadan
Department of Industrial Engineering, German Jordanian University, Mushaqar, 11180, Amman-Jordan E-mail: saleem.ramadan@gju.edu.jo

ABSTRACT

There has been an increase in the number of countries that encourage companies to use electrical commercial vehicles to reach targets regarding emission of greenhouse gases, therefore, more companies are using electrical vehicles for last-mile deliveries. Unfortunately, these vehicles have limitations regarding battery capacity and consequently limitations on their freight capacity and driving mileage. In this article a two-stage heuristic is proposed for dispatching capacitated multi-vehicle with freight capacity, mileage and time-window constraints. The experimentation performed showed that the proposed heuristic has good performance relative to the performance of the mixed integer programming method.

Keywords: multi-vehicle routing problem (MVRP), capacitated vehicle routing problem (CVRP), time-window, electrical vehicles.

I. INTRODUCTION

Green logistics aims to measure all ecological impacts of logistics including transportation between producers and consumers. The growing interest in green logistics is due to several factors including but not limited to: strict environmental regulations, rising fuel prices and striving to improve market position by marketing the company as green company [1] .

Vehicle routing problems VRPs usually used to describe the distribution tasks of the logistics in the companies. VRPs usually minimize total transportation costs of multiple routes for visiting several customers starting and ending at the depot [2, 3, 4]. Over years scholars developed several extensions for the basic VRP[5, 6, 7] such as capacitated VRP, which is a VRP with limited freight capacity for the truck. Time window constraints VRP, VRPTW, is another widely used extension for the basic VRP in which the truck has to reach the customers in certain time slots [8,9]. For Electrical Commercial Vehicles, ECV, the battery can support limited mileage and hence it can be modeled as VRP with mileage constraint. [10] discussed the mixed fleet VRP problem with ECV and conventional vehicles where the recharging time was calculated based on total distance traveled with the battery and the travel range of the battery. [11] discussed the scheduling problem of the electrical busses with limited battery capacity in which the travel range is limited by the battery capacity.

This article aims to introduce a new heuristic to solve Capacitated Electrical Commercial Multi-Vehicle Routing Problem with Time window, Mileage, and Weight constraints VRPTMWh. This

heuristic minimizes the total delivery time under time window, mileage and weight constraints. The total delivery time is calculated as the overall travel time and service time for all of the trucks used in the delivery.

This article is organized as follows: Section 2 discusses the mixed integer programming formulation for VRPTMW; Section 3 presents the proposed heuristic for VRPTMW, Section 4 discusses the experimentations and results and Section 5 draws concludes.

II. MIXED INTEGER PROGRAMMING FORMULATION

The variables and notations used in the article are as follows:

j and k: are the same indices to represent the nodes

i: index for trucks Djk : is the distance between nodes j and k

Xijk : is a binary variable equals to 1 if arc j, k is traveled by truck i and "0" otherwise

NT: number of trucks available

NJ: number of nodes and is the same as NK

Wk : weigh for node k in lb

NHJ :number of nodes with hard time window Cij : cumulative time for truck i up to node j Wmax i : maximum weight for truck i

Dmax i : maximum mileage for truck i

UTmWj: upper time window for node j LTmWj : lower time window for node j Tm: total delivery time in minutes

AvgSpd: average speed of the truck in km/minute

AvgSrvTm: average unloading time in lb/minute

In this article, the VRPTMW was modeled as a machine scheduling problem with time window constraints to process the jobs and capacity constraints on the machines. The machines in the formulation represent the trucks and the jobs represent the nodes in the routes. The mathematical formulation is as follows:

Objective function:

$$Tm = \sum_{i=1}^{N_T} \sum_{j=0}^{N_J} \sum_{k=0}^{N_K} X_{ijk} \left(\frac{D_{jk}}{AvgSpd} + \frac{W_k}{AvgSrvTm} \right) \qquad (1)$$

The constraints are:

$$C_{i0} = 0 \qquad \forall\, i = 1, \ldots, N_T \qquad (2)$$

$$\sum_{i=1}^{N_T}\sum_{\substack{j=0\\ j\neq k}}^{N_J} X_{ijk} = 1 \qquad ,\forall\ k = 1,\ldots,N_K \tag{3}$$

$$\sum_{i=1}^{N_T}\sum_{\substack{k=0\\ j\neq k}}^{N_K} X_{ijk} = 1 \qquad ,\forall\ j = 1,\ldots,N_J \tag{4}$$

$$\sum_{i=1}^{N_T} X_{ijk} \leq 1 \qquad ,\forall\ j = 0,\ldots,N_J, \quad k = 0,\ldots,N_K \text{ and } j \neq k \tag{5}$$

$$X_{ijk} = 1 - X_{zkj} \qquad ,\forall\ j = 0,\ldots,N_J, k = 0,\ldots,N_K, i = 1,\ldots,N_T, z = 1,\ldots,N_T \text{ and } j \neq k, z \neq i \tag{6}$$

$$\sum_{k=1}^{N_K} X_{i0k} \leq 1 \qquad ,\forall\ i = 1,\ldots,N_T \tag{7}$$

$$\sum_{j=0}^{N_J} X_{ij0} \leq 1 \qquad ,\forall\ i = 1,\ldots,N_T \tag{8}$$

$$\sum_{h=0}^{N_J} X_{ihj} \geq X_{ijk} \qquad ,\forall\ j = 0,\ldots,N_J, k = 0,\ldots,N_K, i = 1,\ldots,N_T, h = 1,\ldots,N_T \text{ and } h \neq j \tag{9}$$

$$C_{ik} + V\ 1 - X_{ijk} \geq C_{ij} + D_{jk}/AvgSpd + W_j/AvgSrvTm \qquad ,\forall\ j = 0,\ldots,N_J, k = 0,\ldots,N_K, i = 1,\ldots,N_T, \text{and } j \neq k \tag{10}$$

$$\sum_{j=0}^{N_J}\sum_{k=0}^{N_K} X_{ijk}\, W_k \leq W_{max_i},\ i = 1, \ldots, N_T, \text{ and } j \neq k \tag{11}$$

$$\sum_{j=0}^{N_J}\sum_{k=0}^{N_K} X_{ijk}\, D_{jk} \leq D_{max_i},\ i = 1, \ldots, N_T, \text{ and } j \neq k \tag{12}$$

$$\frac{C_{ij}}{AvgSpd} \leq UTmW_j,\ i = 1, \ldots, N,\ j = 0, \ldots, N_{HJ} \tag{13}$$

$$\frac{C_{ij}}{AvgSpd} \geq LTmW_j,\ i = 1, \ldots, N,\ j = 0, \ldots, N_{HJ} \tag{14}$$

$$C_{ij} \geq 0 \tag{15}$$

$$X_{ijk} \text{ Binary} \tag{16}$$

Equation (1) calculates the overall total time of the schedule by summing the travel time and the service time for all nodes. Equation (2) sets the cumulative distances for the depot node on all of the routes (trucks) to zero.

Equation (3) and Equation (4) guarantee that each node (other than depot node 0) has only one predecessor and one successor. Equation (5) enforces that an arc cannot be repeated on different trucks. Equation (6) forces the arcs (j,k) and (k,j) to be on the same truck and since k and j can take the value zero (the depot) this equation guarantees the round trip. Equation (7) an Equation (8) are used to force truck i, if used, to go once from the depot and once to the depot. Equation (9) guarantees that the predecessor for node j and the node j itself are on the same truck. Equation (10) calculates the cumulative time from node k taking into consideration the service time.

Equation (11) represents the weight constraint of the truck. Equation (12) represents the mileage constraint of the truck. Equation (13) and equation (14) ensure that the time window constraints are met for those nodes that have hard time windows.

III. PERFORMANCE MEASURES

The performance of the proposed heuristic was measured using Relative Error percentage RE% measure. RE% is the difference between the total travel time found by the heuristic T_{mh} and the total travel time of the optimal schedule Tmop found by the mathematical model solved by CPLEX relative to T_{mop} . RE%, given by Equation (17), can only be used when T_{mop} is available and its value is more than zero.

$$RE\% = \frac{TT_h - TT_{op}}{TT_{op}} 100\% \qquad (17)$$

The proposed heuristic

The VRPTMWh heuristic consists of two heuristics, one construction heuristic and one improvement heuristic. The pseudo-code for the construction heuristic is as follows:

- Create a list of all nodes N
- Calculate the values of the overall time matrix OT by adding the time to travel between nodes j and k and the time to unload the freight for node j, W .
- Create a list of hard time nodes SHTWN
- Sort SHTWN ascending wise based on their UTmW values
- set i=0
- Do while SHTWN set is not empty
- set i=i+1

- create cluster i as follow: include the first node in SHTWN in the cluster and add the nodes with the smallest Overall time OT from N such that the time window for the hard time node in the cluster is not violated and the weight and mileage constraints for truck i are not violated.
- update N and SHTWN by removing the selected nodes from N and SHTWN
- End while
- if N is not empty
- put the remaining nodes in cluster i+1 in the same order that they appear in N
- set flag = 1
- else form routes by assigning the nodes in each cluster to the corresponding truck in the same order that they appear in the cluster
- End if

The improvement part heuristic will not be invoked unless there is a cluster which doesn't include any node from SHTWN, i.e., if flag=1. The pseudo-code for the improvement heuristic is as follows

- if flag = 1
- calculate the mileage, weight and distance from the last node in the cluster to the depot for each cluster other than cluster i+1
- for all nodes in cluster i+1 do the following (indexed g)
- for all clusters other than cluster i+1 do the following (indexed z)
- add the current node g from cluster i+1 to the current cluster z if
- the distance between the last node in the current cluster z and depot plus the distance between the current node g and its successor is more than or equal to the distance between the last node in the current cluster z and the current node g plus the distance between the current node g and the depot
- the weight and mileage constraints for truck z are not violated
- End if
- End for
- End for
- update the cluster pool by removing any empty cluster from the pool
- form routes by assigning the nodes in each cluster to the corresponding truck in the same order that they appear in the cluster
- else
- form routes by assigning the nodes in each cluster to the corresponding truck in the same order that they appear in the cluster
- End if
- report routes

To illustrate how VRPTMWh works, consider 6 nodes of which nodes 1, 2 and 3 have upper hard time windows at 11 AM, 10 AM, 12 PM respectively. This means that the set of nodes N is [1 2 3 4 5 6] and the set of the hard time nodes SHTWN is [2 1 3]. The truck leaves the depot at 8:00 AM. The distance matrix (km) is as follows:

	1	2	3	4	5	6
1	0	8	7	11	10	8
2	8	0	9	6	14	6
3	7	9	0	12	6	11
4	11	6	12	0	10	7
5	10	14	6	10	0	11
6	8	6	11	7	11	0

The distances from the depot for nodes 1 through 6 are 13, 9, 15, 14, 12 and 13 km respectively. The weights for the six nodes are 700, 219,590, 436, 208 and 219 lb respectively. Three trucks are considered with maximum weight of 2000 lb and mileage capacity of 100 km. The average truck speed is 20 km/hr (0.333km/minute) and the unload speed is 500lb/hr (8.33lb/minute).

The resulting values for the overall time matrix OT_{jk} are as follows

	1	2	3	4	5	6
1	70.0	94.0	91.0	103.0	100.0	94.0
2	45.9	21.9	48.9	39.9	63.9	39.9
3	80.0	86.0	59.0	95.0	77.0	92.0
4	76.6	61.6	79.6	43.6	73.6	64.6
5	50.8	62.8	38.8	50.8	20.8	53.8
6	45.9	39.9	54.9	42.9	54.9	21.9

For example $OT_{12} = \frac{8}{0.333} + \frac{700}{10} = 24.0 + 70 =$ 94.0 minutes

Cluster 1 starts with node 2 with a total distance from the depot of 9 km and a total weight of 219 lb. The overall time for this distance and weight is 9/0.33+219/8.33=53.6 minutes. Node 2 will be removed from N and SHTWN. The truck can have more nodes as the weight, mileage and node 2 upper time window constraints are not violate yet. The smallest OT_{jk} node is node 4 with OT_{24} of 39.9 (arbitrary between nodes 4 and 6). Node 4 will be added to the cluster with distance between node 2 and node 4 of 6 km and a freight weight of 436 lb. The total distance now is 15 km and the total weight is 655 lb. The weight and mileage constraints are not violated yet and the upper time window for node 2 also not violated.

The smallest OT_{jk} node for node 4 is node 6 with OT_{46} of 64.6 and hence it will be added to the cluster if the constraints are not violated. The overall distance is 15+7=22 km and the overall weight is 655+219

=874 lb which indicates that the weight and mileage constraints are not violated also the time window constraint for node 2 is not violated so node 6 will be added to the cluster. Node 6 will be removed from N. The smallest OTjk value to node 6 is node 1. If node 1 is added, the overall weight will be 874+700=1574 and the mileage is 22+8=30 , hence the mileage and weight constraints are not violated. The time to reach node 1 will be 874/8.33=104.9 minutes in unloading time plus 30/0.33=90.9 minutes in driving time with total time of 195.8 minutes. The total time will violate the upper time window for node 2 (120 minutes) and hence node 1 will not be added to the cluster. This will end cluster 1. The same procedure applies for cluster 2. Cluster 2 starts with the first node in the updated SHTWN set which is node 1. Node 3 is added to this cluster according to the procedure followed in the first cluster and no other nodes are added as the upper time window constraint will be violated for node 1. After Cluster 2 is constructed, no more nodes are in SHTWN set. So the rest of the nodes in N set will be clustered in a separate cluster to form cluster 3. This will give the flag constant the value 1 and hence the improvement heuristic will be invoked. The result of the construction heuristic is as follows:

Cluster 1: {2, 4, 6}

Cluster 2: {1, 3}

Cluster 3: {5}

The overall time of this schedule is 519.2 minutes. After forming the initial schedule by the construction part of the heuristic, the improvement part of the heuristic is applied to fine tune the schedule. The nodes in cluster 3 will be redistributed among other clusters if and only if the overall time of the schedule is reduced and the weight and mileage constraints are not violated for the hosting cluster.

The improvement part of the heuristic is guaranteed not to violate the upper time window constraints for any of the hard time window nodes as the nodes will be added after the hard time window nodes in the clusters and cluster 3 does not have any hard time window nodes. Node 5 will be added to cluster 1 as the distance between node 6 and node 5 (11 km) plus the distance between node 5 and the depot (12 km) is less than the distance between the depot and node 5 (12 km) plus the distance between node 5 and the depot (12 km) plus the distance between node 6 and the depot (13km).

The overall saving in the distance is 37-23=14 km which is 14/0.3333=42 minutes. The resulting schedule is: cluster 1 contains nodes {2, 4, 6, 5} and cluster 2 contains nodes {1, 3} with overall time of 477.2 minutes. The optimal solution found by CPLEX is: cluster 1contains nodes {1, 6, 4} and cluster 2 contains nodes {2, 3, 5} with optimal overall time of 471.2. The relative error is RE = 477 $\frac{.2-471.2}{471.2}$ 100% = 1.27%.

IV. EXPERIMENTATIONS AND RESULTS

The data for experimentation was generated randomly as follows: the distance matrix is sampled from I[UN(2,20)]km, the weight from I[UN(100,1000)]lb, number of hard nodes I[UN(0.25*NJ, (0.5NJ)] and the upper time window constraint I[UN(9:00AM, 14:00PM)] where I[.] is the integer part of [.]. The number of available trucks equals the number of hard nodes with 2000 lb weight capacity and mileage capacity of 100 km. The average truck speed is 20 km/hr (0.333km/minute) and the unload speed is 500lb/hr (8.33lb/minute). 12 problems were solved by CPLEX and $VRPTM_{Wh}$. Number of trucks suggested by the heuristic N_{Th}, optimal number of trucks found by CPLEX N_{Topp}, total time found by the construction heuristic T_{mch}, total time found by the heuristic T_{mh}, optimal total time found by CPLEX T_{mop} were recorded for each problem in Table 1.

Table 1: Results for the 12 problems

Prob. #	N_J	N_H	NTh	NTopp	Tm_{ch}	Tm_h	Tm_{op}	RE_h%	RE%
1	15	7	3	2	684.4	624.4	579.4	10%	8%
2	15	3	2	2	705.4	675.4	601.4	4%	12%
3	15	7	3	3	2153.2	2021.2	1996.2	7%	1%
4	12	4	2	2	690.2	642.2	591.2	7%	9%
5	12	5	4	3	674.2	621.2	586.2	9%	6%
6	12	3	2	2	717.4	640.4	576.4	12%	11%
7	10	5	3	3	789.7	745.6	693.4	6%	8%
8	10	4	3	3	810.8	774.8	723.8	5%	7%
9	10	3	3	3	768.8	678.8	610.8	13%	11%
10	50	23	8	N/A	3463.8	2984.8	N/A	16%	N/A
11	75	27	11	N/A	4896.2	4328.2	N/A	13%	N/A
12	100	43	17	N/A	6845.4	5981.2	N/A	14%	N/A

Table 1 shows that in 7 cases out of 9 cases $VRPTM_{Wh}$ was able to find the optimal number of trucks and for the other two cases (problems 1 and 5) the heuristic missed by only one truck. This means that $VRPTM_{Wh}$ can reasonable used as a prediction tool for the number of trucks needed. Moreover, the RE% values showed that the maximum error committed by $VRPTM_{Wh}$ is 12% while the minimum was 1% with an average RE% of 8%. This again shows that $VRPTM_{Wh}$ can be used to predict the optimal schedule with good accuracy. The REh% shows the effectiveness of the improvement heuristic. The improvement heuristic was able to improve the results of the construction heuristic up to 16% with an average improvement of 10%.

Furthermore, the importance of such a heuristic comes from the fact that CPLEX was unable to solve problems beyond 15 nodes due to memory limitations. With 15 jobs number of constraints was 7505, number of variables was 1376 and number of non-zero coefficients was 38245. These huge numbers are expected as VRP is well known to be an NP-hard problem hence exact solution for such mixed integer programming is not feasible for large number of nodes because of memory limitations an

computational times. This matter renders the exact solutions using mathematical modeling not feasible in most of real life problems and hence shows the importance of using near optimal solution methods like this heuristic.

V. CONCLUSIONS

This article introduced a two-stage heuristic, construction heuristic followed by an improvement heuristic, to dispatch a capacitated multi-vehicle routing problem with capacity, mileage and upper time-window constraints. The experimentation performed showed a good performance for the proposed heuristic. The results showed that the proposed heuristic is best used with problems with large number of nodes as the solution for the mixed integer programming in this case is characterized by high computational time and memory limitation. Moreover, the results showed that the heuristic can be used to predict the number of trucks needed in the dispatch process with good accuracy.

REFERENCES

[1] Dekker, Rommert & Bloemhof, Jacqueline & Mallidis, Ioannis, 2012. "Operations Research for green logistics – An overview of aspects, issues, contributions and challenges," European Journal of Operational Research, Elsevier, vol. 219(3), pages 671-679.

[2] Cordeau, J.-F.; Savelsbergh, M.W.P.; Vigo, D. Chapter 6 Vehicle Routing. In Handbooks in Operations Research and Management Science; Elsevier: New York, NY, USA, 2007; Volume 14, pp. 367–428.

[3] Li JQ, Borenstein D, Mirchandani PB. A decision support system for the single-depot vehicle rescheduling problem. Computers & Operations Research. 2007 Apr 30; 34(4):1008±32.

[4] Narasimha KS, Kumar M. Ant colony optimization technique to solve the min-max single depot vehicle routing problem. InAmerican Control Conference (ACC), 2011 2011 Jun 29 (pp. 3257±3262). IEEE.

[5] Anbuudayasankar SP, Ganesh K, Mohapatra S. Survey of methodologies for tsp and vrp. InModels for Practical Routing Problems in Logistics 2014 (pp. 11±42). Springer International Publishing.

[6] Ai TJ, Kachitvichyanukul V. Particle swarm optimization and two solution representations for solving the capacitated vehicle routing problem. Computers & Industrial Engineering. 2009 Feb 28; 56(1):380±

[7] Toth and D. Vigo. The granular tabu search and its application to the vehicle-routing problem.

[8] INFORMS Journal on Computing, 15(4):333{346, 2003.

[9] Gendreau and C. D. Tarantilis. Solving large-scale vehicle routing problems with time windows: The

[10] state-of-the-art. Technical report, CIRRELT-2010-04, 2010.

[11] Daneshzand F. The vehicle-routing problem. Logistics Operations and Management. 2011 May 25; 8:127±53.

[12] Gon_calves, S. R. Cardoso, Relvas S., and A. P. F. D Barbosa- P_ovoa. Optimization of a distribution network using electric vehicles: A VRP problem. Technical report, CEG-IST, UTL, Lisboa, 2011.

[13] Wang and J. Shen. Heuristic approaches for solving transit vehicle scheduling problem with route and fueling time constraints. Applied Mathematics and Computation, 190(2):1237{1249, 2007.

Modeling and Control of Automatic Ball - Shaped Tapioca Pearls Forming Machine

[1] Wu- Sung Yao, [2] Ping- Miao Chen, [3] Mei- Ling Tsai, [4] Ya- Ling Yang

[1]Department of Mechanical and Automation Engineering, National Kaohsiung University of Science and Technology,(NKUST)

[2]Department of Mechanical and Automation Engineering, NKUST

[3]Department of International Business and Trade, NKUST

[4]Department of Cultural and Creative Industries, NKUST

E-mail: [1]wsyao@ nkust.edu.tw

ABSTRACT

A novel mechanism for automatic forming of the tapioca pearls is presented in this paper with analytical and experimental studies. A system modeling and control technique are adopted for the forming machine driven by two servo motors. One servo motor is used to force two parallel cylinder rollers to do roll motion. The other motor is used to control the gap between the two rollers. Through the synchronous control of the two motors, the required ball size of the tapioca pearls can be achieved. The precise synchronous control of the two motors is the key point. Therefore, an accurate system mathematical model is given for the proposed system. A synchronous control scheme is adopted then applied to the model obtained using the proposed technique. The simulated and experimental results substantiate the constructed system model and demonstrate the effectiveness of the control scheme.

Keywords - Automatic Tapioca Pearls Forming Machine, Synchronous Control, System Modeling.

I. INTRODUCTION

Ball-shaped foods such as tapioca balls, pearl balls, fish balls and meat balls are very common. These ball-shaped foods are usually manually prepared by kneading. The preparation is time consuming and labor intensive, and thus it is not conducive to mass production. To increase production efficiency and reduce production cost, it is a trend to produce processed foods by automated machines. Thus there is a need to provide a ball-shaped food processing machine with good processing speed and low error rate.

The massing and sizing of the particles are the most important unit operations in the production of different sized ball-shaped foods. For example, the Tapioca pearls typically have a size ranges from 1.0 to 9.0 mm depending on the requirements. As shown in Fig. 1, the Tapioca pearl size is mainly affected by the feeding rate and the gap of the two ball-shaped rollers driven two motors, where the drive for the ball-shaped rollers is called the roller motor and the drive for the gap of the two rollers is called the gap motor. The objective of this work is to focus on, through the synchronous control of the two motors, the required ball size of the tapioca pearls can be varied. The precise synchronous control of the two motors is the key point. Therefore, an accurate system mathematical model is given for the proposed system. The capability of the automatic tapioca pearls forming machine to accurately form the tapioca pearls is an important requirement. Synchronous control schemes for the two motors that are capable of

achieving required size of the tapioca pearls are particularly important for this application. The coordination of two drive axes is often achieved by decoupling the commands to each of the drive. It is assumed implicitly, by such an approach that, the servomechanisms of individual drives ensure accurate tracking of the axis command inputs. A general synchronous control scheme [1-4] is the parallel synchronous control technique [2], in which the loop controllers of each individual axis are designed independently. However, for control of a parallel motor pair, it is demanding for both control performances of the motors to respond identically to the same commands, particularly with the presence of the mechanical coupling.

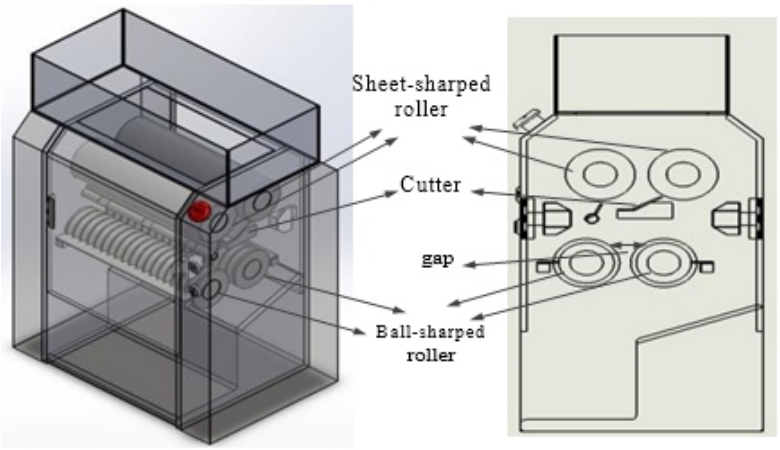

Fig. 1. Configuration of Automatic Ball-Shaped Tapioca Pearls Forming Machine

Another synchronous control scheme is called the tandem control [5], i.e., the simplified master-slave control, where the reference input for the slave axis is generated based on the measured master axis position and the desired contour. The master-slave control was first proposed and applied to a biaxial system by Sarachik and Ragazzini [6]. A feed forward gain can be added to improve the system transient response. The above-mentioned approaches are commonly applied to multi-axis motion control systems. An accurate model of the controlled plant is important for the design of the synchronous control, particularly with the presence of the mechanical coupling. In the many control cases without mechanical coupling, the individual motor modeling should be the only consideration prior to control design. However, with the coupling effect, it is necessary for the control technique to precisely synchronize the positions of the two parallel motors, for not only precision positioning but also prevention of any possible hardware damage.

This paper is organized as follows. In Section II, the mathematical model for the parallel linear servo system is constructed. Section III discusses the proposed identification technique applied to synchronous control. The experimental studies are presented in Section IV, followed by Section V, which briefly concludes the paper.

II. SYSTEM MODELING

The paper is aimed to provide a modeling and control method for ball shaped food processing machine. The main components of the machine are two ball-shaped food forming, where a plurality of the ball-shaped gaps are defined between the two rollers. Thereby, a food slug can be efficiently formed into ball- shaped food. Therefore, the control system with the two parallel cylinder rollers driven two motors can be modeled as shown in Fig. 2. Based on the Fig. 2, the dynamic modeling can be given as

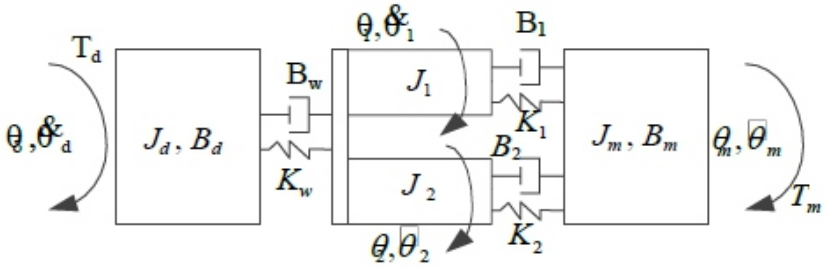

Fig. 2. Modeling of the machine in Fig. 1

$$J_d\ddot{\theta}_d + B_d\dot{\theta}_d + B_w\left(\dot{\theta}_d - \dot{\theta}_m\right) + K_w\left(\theta_d - \theta_m\right) = T_d$$

$$d = p\,\theta_d$$

where the parameters of the system modeling are listed in Table 1.

q_1	rotation angular displacement of ball-shaped roller 1
q_2	rotation angular displacement of ball-shaped roller 2
qm	rotation angular displacement of the roller motor
qd	rotation angular displacement of the gap motor
Tm	torque input of the roller motor 1
Td	torque input of the gap motor
Tw	load torque due to the gap varying of the two rollers
$J1$	equivalent inertia of ball-shaped roller 1
$J2$	equivalent inertia of ball-shaped roller 2
Jm	equivalent inertia of the roller motor
Jd	equivalent inertia of the gap motor
Bm	equivalent damping of the roller motor
Bd	equivalent damping of the gap motor
$B1$	equivalent damping of the coupling between roller motor and the ball-shaped roller 1
$B2$	equivalent damping of the coupling between roller motor and the ball-shaped roller 2
Bw	equivalent damping of the coupling between the ball-shaped rollers and the gap motor
$K1$	equivalent stiffness of the coupling between roller motor and the ball-shaped roller 1
$K2$	equivalent stiffness of the coupling between roller motor and the ball-shaped roller 2
Kw	equivalent stiffness of the coupling between the ball-shaped rollers and the gap motor
d	gap of the two rollers
p	pitch between the d and qd

Table 1 Defined Parameters of the Gimbal System

$$J_m \ddot{\theta}_m + B_m \dot{\theta}_m + B_1 \left(\dot{\theta}_\mu - \dot{\theta}_1 \right) + B_2 \left(\dot{\theta}_\mu - \dot{\theta}_2 \right) + K_1 \left(\theta_m - \theta_1 \right) + K_2 \left(\theta_m - \theta_2 \right) = T_m$$

$$J_1 \ddot{\theta}_1 + B_1 \left(\dot{\theta}_1 - \dot{\theta}_m \right) + K_1 \left(\theta_1 - \theta_m \right) + B_w \left(\dot{\theta}_\mu - \dot{\theta}_s \right) + K_w \left(\theta_m - \theta_d \right) = 0$$

$$J_2 \ddot{\theta}_2 + B_2 \left(\dot{\theta}_2 - \dot{\theta}_m \right) + K_2 \left(\theta_2 - \theta_2 \right) + \left(B_w \left(\dot{\theta}_m - \dot{\theta}_d \right) + K_w \left(\theta_w - \theta_d \right) = 0 \right.$$

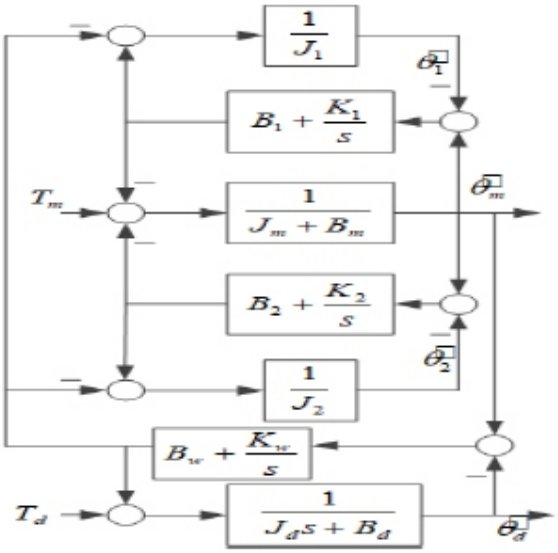

Fig. 2 Block diagram of the target system from the thrust input to velocity output with the mechanical coupling.

Through the Laplace transformation of (1), its block diagram can be given as shown in Fig. 2, where Ωm / Ωd and T%m / T%d are the Laplace transformations of θ&m / θ&d and Tm / Td respectively.

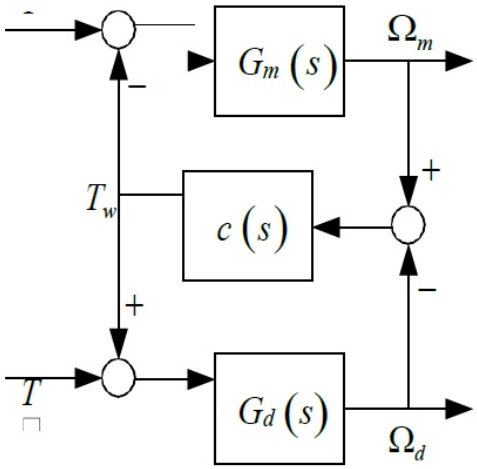

Fig. 3 Block diagram of the target system from the thrust input to velocity output with the mechanical coupling.

The controlled plant can be simplified as shown in Fig. 3, where Gm (s) represents the transfer function for the torque input T_m to the rotation velocity output Ω_m of the roller motor and G_d (s) is that for the gap motor. The torque T_w is caused by the deformation of the mechanical coupling due to non-synchronization of the two motors and can be defined as $T_d = c\ (s)(\Omega_m - \Omega_d)$. c (s) represents the dynamic behavior of the mechanical coupling. In Fig. 3, the following transfer functions can be obtained with $T_d = 0$

$$\frac{\Omega_m}{T_m} = \frac{G_m(1+cG_d)}{1+cG_m+cG_d}, \text{ and } \frac{\Omega_d}{T_d} = \frac{cG_mG_d}{1+cG_m+cG_d} \qquad (2)$$

Similarly, for $T_m = 0$

$$\frac{\Omega_m}{T_d} = \frac{cG_mG_d}{1+cG_m+cG_d}, \text{ and } \frac{\Omega_d}{T_d} = \frac{G_d(1+cG_m)}{1+cG_m+cG_d} \qquad (3)$$

As illustrated in Fig. 3 and indicated in (2) and (3), as one motor is mechanically coupled to the other, its dynamic behavior is influenced by the mechanics of the coupled system, i.e., the mechanical coupling and the other motor. The equivalent linear system model studied here is a topic of considerable practical interest, which is motivated by the insight into the system representation allows for a more efficient means of analysis. Therefore, the principle of superposition is adopted to determine the system model in this paper. The model in Fig. 3 can be transformed into the form shown in Fig. 4, in which the mathematical model for the thrust inputs to the velocity outputs is linearly composed of the four transfer functions P_{11} (s) , P_{22} (s) , P_{12} (s) , and P_{21} (s) . Therefore, we have

$$\begin{bmatrix} \Omega_m \\ \Omega_d \end{bmatrix} = \begin{bmatrix} P_{11} & P_{12} \\ P_{21} & P_{22} \end{bmatrix} \begin{bmatrix} T_m \\ T_d \end{bmatrix} \qquad (4)$$

where

$$P_{11}(s) = \frac{G_m(1+cG_d)}{1+cG_m+cG_d} \qquad (5)$$

$$P_{12}(s) = \frac{cG_mG_d}{1+cG_m+cG_d} \qquad (6)$$

$$P_{21}(s) = \frac{cG_mG_d}{1+cG_m+cG_d} \qquad (7)$$

$$P_{22}(s) = \frac{G_d(1+cG_m)}{1+cG_m+cG_d} \qquad (8)$$

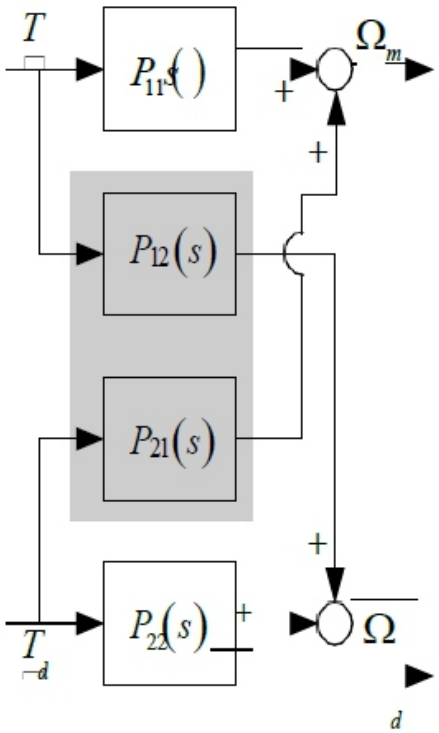

Fig. 4 Control system linearly composed of the four transfer functions

The system diagram shown in Fig. 4 can be used to represent the model of Fig. 3. Although the four transfer functions in (5)-(8) can be measured by an dynamic interactions described with a linear representation. Although the nonlinear nature may need to be recognized, in many cases a linearized open-loop identification, it is preferable that they are determined by a closed-loop identification method for the required accuracy with disturbances, and this leads to an indirect modeling process. In this technique, the open-loop identification as indicated in Fig. 4 is replaced by the velocity closed loop identification shown in Fig. 5, where C_m (s) and C_d (s) are the given velocity controllers for motor 1 and motor 2, respectively. The controllers have been well designed to stabilize the system, and they are C_m (s) = 0.025 + 2.5 s and C_d(s) = 0.032 + 3.2 s . The measured frequency response of the velocity closed loop will be used to determine the transfer function of the thrust input to the velocity output for the coupled system.

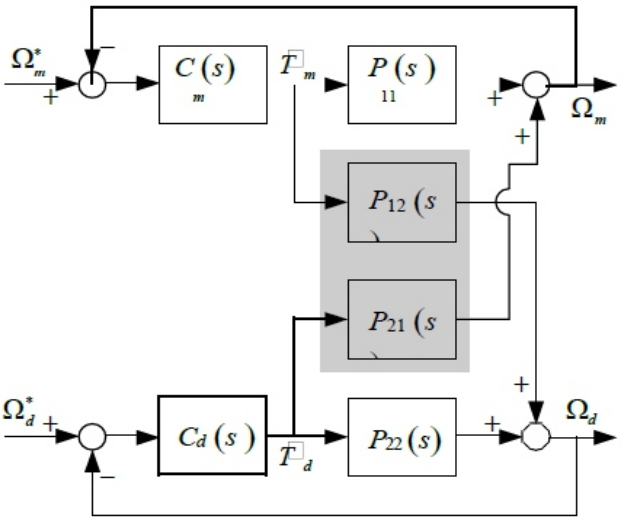

Fig. 5 The control system with the velocity controllers

A practical identification measurement for modeling the investigated system is given. The gap motor is not actuated and is passively dragged to move by the roller motor via the coupling. The roller motor is fed with a swept sine velocity command Ω_m to drive the entire system, including the two rollers and the mechanical coupling. By measuring the velocity output signals of the gap motor and the roller motor, i.e., Ω_m and Ω_d in Fig. 8, the transfer functions from * to Ω and * to Ω can thus be obtained with curve fittings, as the result presented in (9) and (10), respectively. Equation (10) includes the dynamics characteristic of the mechanical coupling. Repeating the procedure, the gap motor is actuated while the roller motor is free motion so that the transfer functions of * to Ω and * to Ω_m can be obtained, as given in (11) and (12), respectively. Frequency responses obtained from simulation and experiment of (9)-(12) is shown in Fig. 6. The velocity controllers for closed-loop identification, i.e., C_m (s) and C_d (s) are included in the transfer functions listed in (8)-(11) and should be extracted to determine the required transfer functions of $P_{11}(s)$, $P_{22}(s)$, $P_{12}(s)$, and $P_{21}(s)$.

This will be detailed in the following.

$$G_{\Omega_m^* - \Omega} (s) = \frac{1110}{s^2 + 28s + 1110} \quad (9)$$

$$G_{\Omega_m^* - \Omega} (s) = \frac{1366}{s^2 + 28s + 1366} \quad (10)$$

$$G_{\Omega_d^* - \Omega} (s) = \frac{3815}{s^3 + 57s^2 + 1759s + 38149} \quad (11)$$

$$G_{\Omega_d - \Omega_m} (s) = \frac{38619}{s^3 + 55s^2 + 1689s + 38619} \quad (12)$$

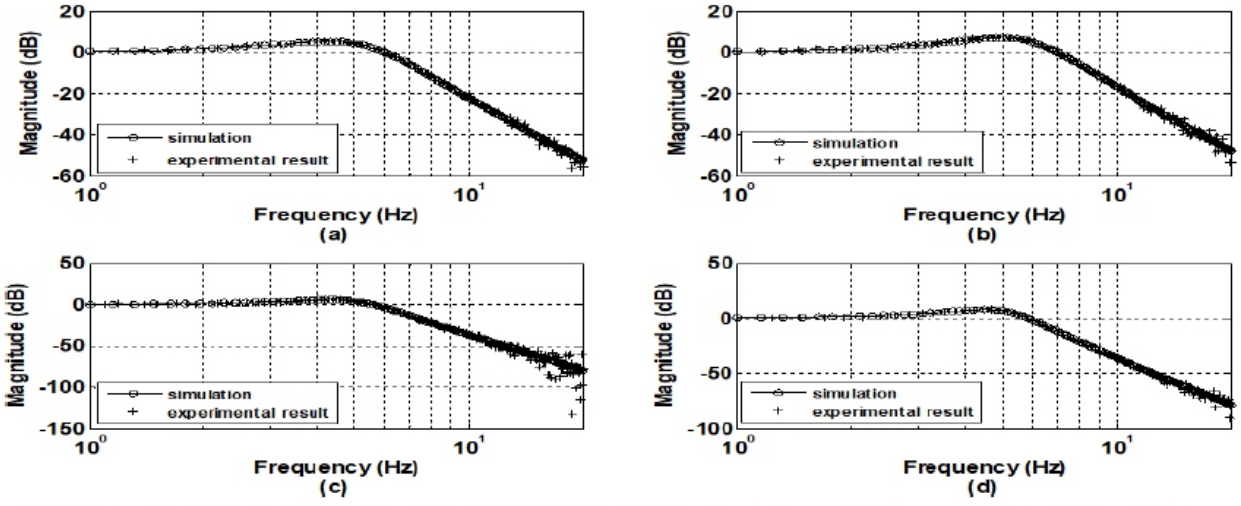

Fig. 6 Frequency responses obtained from simulation and experiment of (a) $G_{\Omega_m^* - \Omega_m}$, (b) $G_{\Omega_m^* - \Omega_d}$, (c) $G_{\Omega_d^* - \Omega_m}$ and (d) $G_{\Omega_d^* - \Omega_d}$.

II. EXPERIMENTAL STUDIES

To verify the proposed identification technique, this paper adopts the compliance control technique, where position control is applied to the gap motor, and the roller motor is given by the velocity control

loop. The proposed control scheme is shown in Fig. 7, where $C_{dd}(s) = 2$ is the position loop controller, Φ is the position output, and d ∗ is the position command input. Note that the pitch p = 0.5mm rev is given in this case. The drivers of the motors are set to the torque control mode to fit the system modeling and control design. The command voltage ranges between -8 and +8 V produced by the controller, a TMS320C32 digital signal processor (DSP) for real-time computation. The commands of Ω∗ = 350rpm and d ∗ = 9mm can be determined by the material characteristics and its required diameter of the ball-shaped tapioca pearls. The experimental results shown in Figs. 8 and 9 can be used to verify the effect of the proposed modeling method and the control scheme.

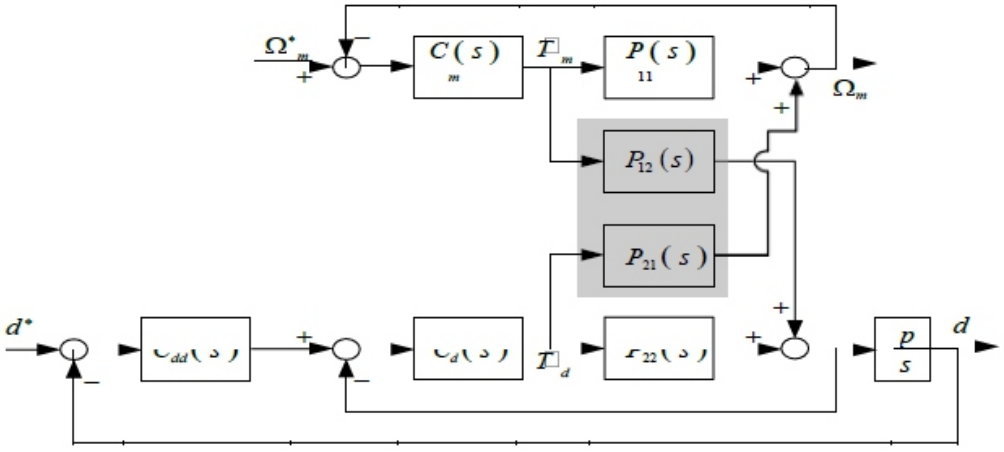

Fig. 7 The proposed synchronous control structure.

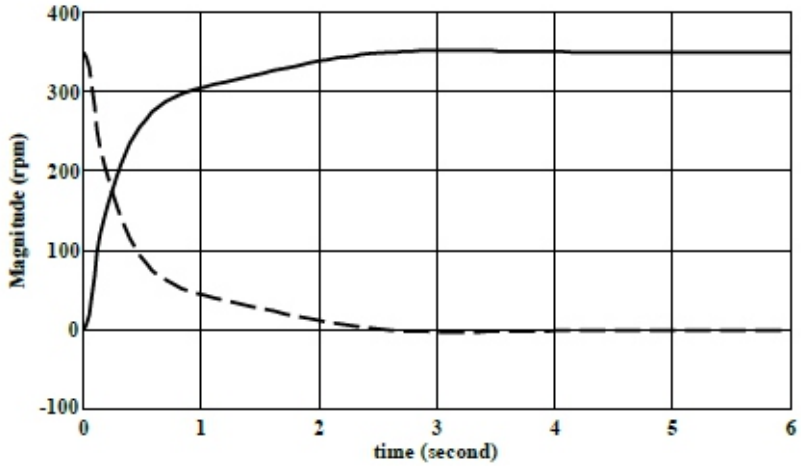

Fig. 8 Velocity (solid-line) and error (dashed-line) response of the roller motor

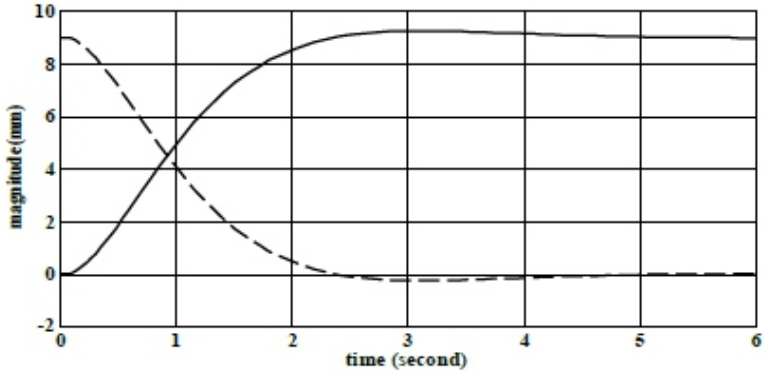

Fig. 9 Position (solid-line) and error (dashed-line) response of the gap motor

III. CONCLUSION

This paper has successfully developed a system modeling technique for an automatic ball-shaped tapioca pearls forming machine, where the model for the mechanical coupling has been identified. The model constructed from the multi-variable system identification method has been verified by comparing the simulation results with the experimental results. Based on the model, a compliance synchronous control scheme has been given for the machine. The experimental results showed that the modeling is effective. It can be concluded that a required performance can be achieved with the proposed system modeling and synchronous control techniques.

REFERENCE

[1] Sun, D., Dong, H. N., and Tso, S. K., 2002, "Tracking stabilization of differential mobile robots using adaptive synchronization control," Proceedings of IEEE International Conference on Robotics and Automation, Vol. 3, pp. 2638 - 2643.

[2] Yao, W. S., 2002, "Design of Linear Servo Systems for High Speed Machine Tools," Dissertation for Doctor of Philosophy, Department of Mechanical Engineering, National Cheng Kung University, Taiwan.

[3] Lammers, G. M., 1994, "Linears lead in ultra-smooth motion," Machine Design, pp.60-64.

[4] Zhao, D., Li, S., Gao, F., and Zhu, Q., 2009, "Robust adaptive terminal sliding mode-based synchronized position control for multiple motion axes systems," Control Theory & Applications, Vol. 3, pp.136-150.

[5] FANUC AC SERVO MOTOR (α)-series, FANUC, Japan, December, 1999.

[6] Sarachik, P. and Ragazzini, J. R., 1957, "A 2-dimensional feedback control system," Transactions of the AIEE, Vol. 76, pp. 55-61.

New Methods and Approaches to Treatment High- Manganese Steel Cone Crusher

[1] Nazieh N. H., [2] Osinniy V. Ya, [3] Makeiev S. Yu. [4] Holyavik O. V., [5] Osinnja N. V.

[1]Mechanical Engineering Department, Zarqa University, Jordan

[2, 3, 5]Department of Mineral Mining at Great Depths, M.S. Polyakov Institute of Geotechnical Mechanics under the National Academy of Sciences of Ukraine

[4]Department of Mechanics of Plasticity of Materials and Resource-Saving Processes, National Technical University of Ukraine "Igor Sikorsky Kyiv Polytechnic Institute", Institute of Mechanical Engineering (I. Sikorsky KPI), Kyiv, Ukraine

E-mail: [1]nhasan@zu.edu.jo, [2]osennjaja@ukr.net, [3]smakeev@ukr.net, [4]k_omd@ukr.net, [5]osennjaja@ukr.net,

ABSTRACT

The work is devoted to experimental researches influence of low-temperature plasma on the surface layer armored cones crusher bowl in plasma-mechanical treatment. It is established that the direct action plasma torches does not comply with the requirements of uniform thermal heating of the cutting zone and needs to be replaced with plasma torches indirect actions.

Keywords - Plasma, Manganese Steel, Cone Crusher, Flux Density Energy in the Anode.

I. INTRODUCTION

Many important elements of mechanical engineering structures during their operation in the mining industry are in serious extreme conditions. Such conditions include stationary and moving armor cone crushers (Fig.1 position 20 and 7).

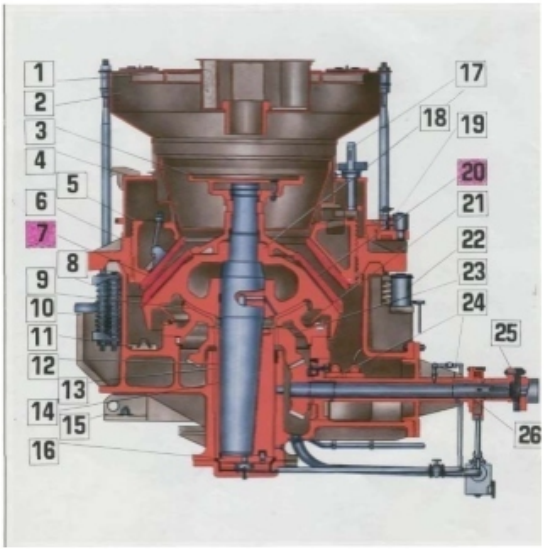

Fig. 1. KSD-2200 conecrusher

Cone crushers are featured by large enterprises in the mining and aggregates industry not only in Ukraine but also in other countries of the CIS (former Soviet Union). Processing plants in Krivoy Rog

cone crusher coarse, medium and fine crushing are used more than half a century. This is due to the homogeneous high- quality crushing of iron ore, the ease of maintenance of the crusher in operation. Work surfaces armored cones crusher bowl work in extreme conditions, constantly being subjected to impact-abrasive wear. Casting cones are made of highly manganese steels G13L 110 having a high capacity for work hardening in the process of cold plastic deformation. By more pressure in the crushing process of strong ores, high wear resistance in them combined with good ductility. Casting highly manganese wear resistant steels requires high production culture. Any deviation from the technology may lead to cracking or destruction in the manufacturing process, and especially during operation. At high manganese content (over 10%) 110 steel G13L under the action of the cutting forces becomes the tendency to hardening, resulting in dramatically increases the strength, decreases the ductility of the surface layer, the austenite partially transferred to the martensite.

The increase in material strength of the workpiece reduces the cutting speed, since such changes in mechanical properties accompanied by the increase of wear of the cutting edges of the cutters, intense wear of the tool until it breaks. Low thermal conductivity and thermal diffusivity high-manganese steels, difficult heat removal from the cutting edge of the cutter require raising the temperature of the surface layer of workpiece before cutting. To intensify the cutting process when machining armor cones crushers technologists of machine-building enterprises use artificial heating of the shear layer of the workpiece to a certain temperature with the help of plasmatrons of direct action. The process of plasma-machining (PM) includes heating the surface layer of the workpiece before the cutter with air plasma arc to a temperature close to the melting point of the base metal and the subsequent removal of the cutter of this layer.

Based on a generalization, formulated by the author [1] friction in the region of the cutter blades on the workpiece is three-stage process that combines the interaction of the mating surfaces, structure evolution and destruction of these layers. The author suggests that stress is localized in spots touch and leads to the accumulation of deformation in the layer under the friction surface, the formation of microcracks and destruction of this layer. In [2] noted that the friction surface and in a surface layer of the material are temperature fluctuations and mechanical stresses, and the plastic shear acts lead to birth in the material of the workpiece elastic shear wave that extends deep into the workpiece with a speed corresponding to the speed of transverse sound waves.

We would like to note that the essence of the plasma- mechanical effects process is that the metal workpiece is the anode of the arc that is stabled flow of plasma generated by the plasma torch designed for cutting metals. In carrying out the PM the temperature of processed armour cone crusher increases, which creates uneven constantly changing, the stress-strain state.

The flow of hot gases contained in the plasma arc, due to the saturation of these gases having high kinetic energy, surface layers, in particular hydrogen. According to author of [3] hydrogen, even in the austenitic structure, can play a negative role on the surfaces of the heated arc, the probability of cracking is extremely high.

Industrial plant for PM armor cones crushers is a set of equipment including lathe model 1540 with faceplate diameter 4 m, power supply APR-404 NF4 for automatic air-plasma metal cutting, plasma torch – PVR-402 NF4, as well as a number of additional devices, including binding mechanism of the plasma torches, the systems for water and gas supply, ventilation, the node auto-protection of the current collector with brushes to power two torches, control panel installation. The face plate with a diameter of 4m to put the workpiece in the center is very difficult, besides the casting has a nonuniform margins that causes roughing with interrupted cuts with high impact loads on the cutting tool. Arise throws currents from 300 A to 400 to 450 A and this causes the creation of a center of the arc spots on the anode (workpiece) stress raisers and cracks. To avoid the appearance of stress raisers and to improve the quality of the processed material and extend the wear of cutting tool has been applied to the plasmatron with magnetic arc control (Fig. 2).

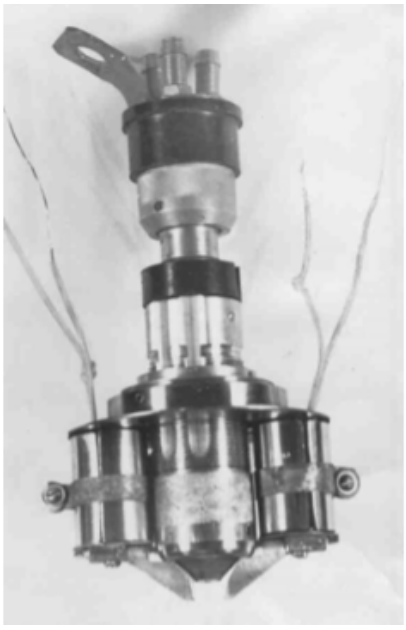

Fig. 2 – PVR402U4 Plasmatron with magnetic arc control

To the treatment of conical workpieces requires the creation of a uniform thermal loads in the cutting zone armor. On the one hand this will reduce the effect of stress concentrators and to improve the quality of the processed material, and on the other hand to increase durability of the cutting tool.

The purpose of work is study, synthesis of temperature characteristics of the plasma arc of the plasma torch direct action and justification of the transition to mechanical treatment of cones crushers the

plasma torches indirect actions with non-toxic plasma jet and plasma-forming gas, that is superheated steam.

II. MATERIAL AND RESEARCH RESULTS

In [4, 5] the authors demonstrated the expansion of technological possibilities of arcs by increasing the width of the warmed layer due to field arcs interacting with a transverse alternating magnetic field. The presence of this field changes the drift of charged particles in an electric field, the ratio of the transfer, the nature of the binding and causes it to move. Imposing on the plasma arc of a transverse magnetic field leads to the deviation of the arc and allows to more evenly heat the area destructible armour layer in front of the cutting edge of the cutter. The angle of deflection of the plasma arc is determined by the operation mode parameters of plasma torch and control the magnetic system. Characteristics that define the interaction of an arc with a transverse variable magnetic field is changed in the following ranges: arc current I = 100 to 400 A, arc length L = 14-50 mm, magnetic induction B = 0- 0,01 TL. The experiments were performed using a rotating partitioned sensor is partially described in [6].

This allowed for roughing cones to increase the performance of heating the workpiece uniform heating of manganese steel along the entire cutting edge of the cutter, and during each period of oscillation of the arc to adjust its capacity by changing the arc current in accordance with the pattern $I = I0+(0,75\div0,85)I0\sin2\beta\max \sin(2\omega t-\pi/2)$ where I0 – the average value of the arc current, Amps; βmax – maximum deflection angle of the arc in a magnetic field, radians; ω – circular frequency of the magnetic field under the action of which arc performs oscillatory motion, radians/sec; t – time, sec; π/2 – the initial phase of oscillations, radian.

On the one hand, we get rid of the stress raisers, and with another – the system is complicated. Chips removable cutter often began to curl around the controlled coils. The specialists had to refuse from this system.

As a result of experiments it is established that the greatest influence on the energy flow in the anode provides an electric current of the arc. With increasing current the energy flow in the anode increases faster than linearly. Strong influence of current due to a change in the characteristics of the plasma flows. In particular, temperature, dynamic pressure and speed of the plasma flow incident on the anode are increasing, and their profiles become broader. The analysis of criterial equations of heat exchange shows that with increasing values of the temperature and velocity coefficient of heat transfer between the plasma flow and the surface of the anode increases. Consequently, the energy flow increases.

For practical purposes, the importance of studying the distribution of the energy flow q on the anode as cone crusher, connects with a prediction and calculation of temperature in the workpiece material (armor), depth of penetration, size of heat affected zone, the mass of the evaporating metal.

The effect of arcing on the distribution density of the energy flux at the anode is considered by the example of air plasma arc. Study of the influence of the gas flow that stabilizes the arc column in the discharge space and the flow of energy generated in the discharge, on the distribution of heat flux density q at radius r is made when the air flow is G = 0.5 and 2.0 g/s, the distance from the cathode to the nozzle exit of the plasma torch h = 4.5 mm and the nozzle diameter d = 6 mm (Fig.3).

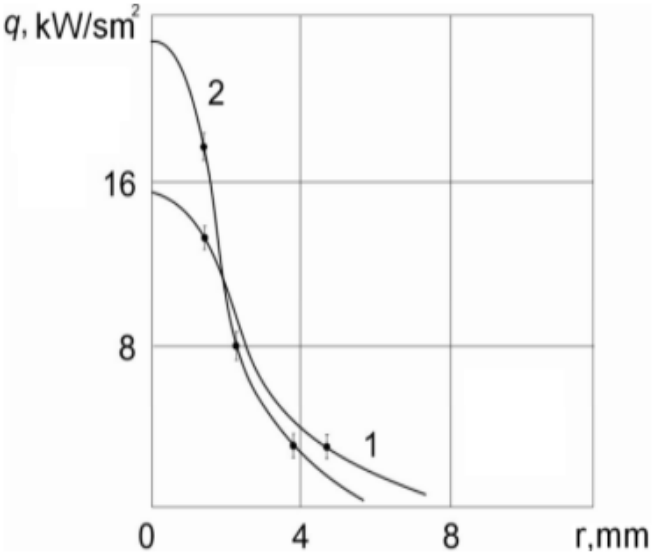

1 – G = 0,5 g/s; 2 – G = 1,0 g/s, I = 200 A , L = 10 mm, h = 4,5 mm, d = 6 mm.

Fig. 3. Radial distribution of heat flux density at the anode and air arcs at different airflows

With the increase of gas flow that stabilizes the arc, the voltage drop across the arc increases, the luminous diameter of the arc and the flow of energy in the anode is reduced.

Distribution of the density of energy flow in the anode spot of the arc air are summarized by the dependence [7].

$$q® = 3,2·10–3Error!exp(–2,6·10–4Error!r2)$$

Deviation of calculated values of q from experimental is 35%. For values of the radius, where $q \leq 0,2 \cdot qmax$ is the deviation of the calculated values of q greater than 35%. However, this is not significant, as the proportion of energy flow entering the anode from outside the circle of this radius is less than 0.25 of the total energy flux to the anode.

Research of the influence of electric current density distribution of the energy flux q is performed at currents of 100, 200 and 300 A (Fig. 4). It was established experimentally that with increasing current the maximum value of the density of energy flow qmax, and the half-width of the q distribution increase. With increasing current and at constant other parameters visually and the photographs, there is an increase of luminescence intensity of the arc column and increase the light diameter. For the plasmatron modes operation, in which q is determined, the volt-ampere characteristic of the arc increasing. This suggests that the electric power of the arc, depending on current growing.

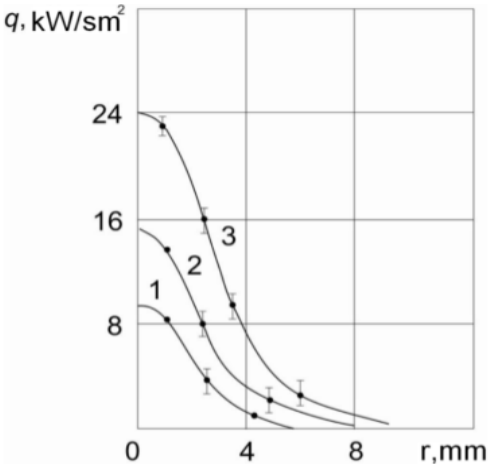

1 – I = 100 A, 2 – I = 200 A, 3 – I = 300 A, L = 10 mm, h = 4,5 mm, d = 6 mm, G =0,5 g/s.

Fig. 4. Radial distribution of flux density energy in the anode of the air arc at different currents

With increasing distance from the cathode to section of the nozzle of the plasma torch the voltage drop across the arc increases, and, consequently, increasing its electric capacity. According to visual observations of the plot arc from the nozzle section of the plasma torch to the anode observed that the opening angle of the plasma flow does not increase with the increasing distance from the cathode to the nozzle section. The density value of the flow of energy and current in the center of the spot with increasing distance from the cathode to the nozzle section decreases (Fig. 5).

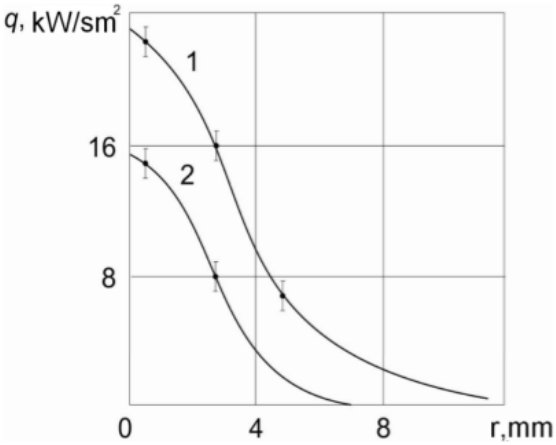

1 – h = 4,5 mm, 2 – h = 6,0 mm, I = 200 A, L = 10 mm, d = 6 mm, G = 0,5 g/s.

Fig. 5. Radial distribution of flux density energy in the anode of air the arc at different distances from the cathode to the nozzle section of the plasma torch

III. DISCUSSION OF THE RESULTS

Plasma heating by open arc cone crushers entails:

- weaken armor being processed in the cutting area;
- the occurrence of local thermal stress field of high intensity and irregularity, which are enhanced by structural transformations occurring in the volume of heated surface layer of manganese steels;
- change of friction parameters on contact surfaces of the cutting edge of the cutter and chips;
- changes in the level of residual stresses in the treated manganese steels;
- usage as a heating of the plasma torch direct action leads to a deterioration of working conditions due to the strong optical radiation.

It should be noted that after heating the armor arc of direct action may stay in basically material the stress raisers and even cracks, which in the operation of crusher factories can reduce the life of the cones.

A significant disadvantage of the plasma technology, using compressed air (plasma gas) is the toxicity of the plasma flows. In the off-gas air plasma jet contains nitrogen oxides, whose concentration is two or more orders of magnitude higher than the permissible sanitary norms that require special devices for removal of polluted gases.

At the turn of the new Millennium the European Union has imposed stringent standards on air emissions, water pollution, waste recycling. According to experts [8] only by developing new cleaning methods and technology, it is possible to implement these standards. Therefore, the development of new plasma processes in various technologies of mining production based on non-toxic low-temperature plasma becomes one of the urgent tasks.

Theoretical and experimental studies of the thermodynamic characteristics of water plasma torches plasma in the temperature range of 2000-6000 K and a pressure of 0.1-0.5 MPa are carried out in Institute of geotechnical mechanics, which showed that the main components of thermally dissociated water vapor are atomic and molecular hydrogen and oxygen, OH radicals. Components of water plasma have no toxic gases [9]. Flow in the inter-electrode gap of high-temperature plasma in the form of superheated steam helps to reduce the negative sound vibrations and effectively solve a few problems: increasing system reliability, reducing the cost of equipment to improve the energy indicators of a plasma jet. In the steam plasma, in which enthalpy is higher than that of air, nitrogen, oxygen and plasma of other gases, and is second only to hydrogen [10].

The thermal conductivity of steam plasma is significantly higher and the viscosity is much lower than in other types of the plasma. Due to this, when burning the arc in the vortex flow of steam-water plasma of the arc column is exposed to not only a strong lateral cooling, in a medium of hydrogen, but also much more intense than in other gases. This in combination with the large specific heat capacity in electric arc plasma torches leads, first, to the large electric field intensity in the arc column, and secondly, to the large enthalpy steam plasma for the same arc current. It becomes possible to build multi- operator systems that work two electric plasma torches (EPT) from a single power supply. Work EPT on the water vaporcan be implemented in two schemes:

1) the external transformation from a separate energy source [11];
2) with internal vaporization due to the energy released in the electrodes of the plasma torch [12].

From the viewpoint of compact design and efficiency, the preference has a scheme in which the formation of steam occurs due to the heat reaching the walls of the electrode from the arc discharge.

IV. CONCLUSIONS

Study of thermomechanical contact interaction when heated by electric arc and mechanical cutting tool superhard materials, in particular, armor cones crushers, showed that the phenomena on the surface of the cutting tool and workpiece material are determined not only by structure and properties of the processed material but also thermodynamic loads from the plasma arc of mechanical shock on the cutter blade.

It was established that in severe working conditions of fixed armor and armor cone crusher bowl on the surface of the contact pieces of ore with armor and in a subsurface layer of armor there are temperature fluctuations and mechanical stresses that cause degradation of the structure of the Hadfield steel. By mechanics that serve cone crusher with many years of experience of their work, it was observed that the wear of the cones (armor) is not all over the surface of the product, and locally in any specific areas. This can be explained by the fact that the base metal after TMO has structural cracks, which during operation of the crusher can also develop prematurely withdraw it from the system.

Based on of the conducted researches it was established that the direct-action plasma torches do not comply with the requirements of uniform thermal heating of the cutting zone and need to be replaced with plasma torches indirect actions.

REFERENCES

[1] I.V. Kragelsky, 1968. Frictionandwear. Mashinostroenie. Moscow.

[2] A.V. Kolubaev, Yu. F. Ivanov, O.V. Sizova, ect. 2008. The effect of elastic excitations on structure formation of the surface layer steel Hatfield by friction. J. technical physics, vol.78, issue 2, 63-70. DOI= http://journals.ioffe.ru/articles/9338

[3] V.I. Panov, 2014. The problems of repair welding of steel 110 G13L large thickness. Welder 1, 36-39. DOI= https://welder.stc-paton.com/ru/welderua/201401

[4] A.F Bulat, V.Ya.Osenniy, and P.V. Bulany, 2007. An experimental study of the curve of the anode in a transverse magnetic field. Geotechnical mechanics, issue 68, 15-23. DOI= http://www.geotm.dp.ua/index.php/en/

[5] V.YA. Osinniy,.,S.YU. Makeiev,N.V. Osinnja, and O.V. Holyavik,2017. Improving the efficiency of plasma-machining manganese steel. New Technologiesand Achievements in Metallurgy and Material Engineering and Production Engineering and Physics: XVIII International Scientific Conference, 01-02.06.2017, Częstochowa: Politechnika Częstochowska, 2017. A collective monograph. Scries: Monografie Nr 68, 329-336. DOI= http://hutnik.wip.pcz.pl/

[6] A.F. Bulat, P. V. Bulany,., and V.Ya. Osenniy, 2003, Control of the heat flux distribution at the anode of a transferred arc argon stabilized and flowing in air, Progress in Plasma Processing of Materials. Eds. P. Fauchais, Begell House. N.Y. Wallingford. 211-218. DOI=http://www.begellhouse.com/journals/4eadd ae7 6bab54e 2.html

[7] M.F. Zhukov, 1979. Principles of calculation of linear-circuit plasma generators. InstituteofThermophysics. Novosibirsk.

[8] J. Amoru,D.Morvan, S.Kavadias, ect. 2005. Control of environmental pollution and treatment processes plasma methods. J. technical physics, vol.75, issue 5, 73-81. DOI=http://journals.ioffe.ru/articles/8552

[9] A.F. Bulat,B.D.Alymov, V.Ya. Osenniy, and L.T Kholiavchenko, 2005.Environmentally-friendly plasma technologies for material processing. In Proceedings of the III International Conference on Problems of nature management, sustainable development and technogenic safety of regions (Dnepropetrovsk, Ukraine, October 03-08, 2005).180-182.

[10] V.YaOsenniy,and N.V. Osinnja,. 2013.About the comparison of the characteristics of electric arc plasma torches with air and water create of plasma. In Proceedings of the XXIII International Conference onDeformation and destruction of materials with defects and dynamic phenomena in rocks and workings (Simferopol, Ukraine, September 23-29, 2013). Taurida national University, 239-242.

[11] A.F.Bulat, I.F. Chemeris, and V.Ya. Osenniy, 2005. The optimization of the steam source parameters for water plasma generators. Geotechnical mechanics, issue 59, 22-28. DOI= http://www.geotm.dp.ua/index.php/en

[12] B.I. Mikhailov, 1991. Physical and technical bases of electric- arc generators of water plasma. Doctoral Thesis. Institute of Thermophysics of SB as USSR. Novosibirsk.

Investigation of Effect of Cutting Parameters on Tool Life in Orthogonal Cutting of AISI316 Stainless Steel

[1] Iman M. Naemah, [2] Yaseen A. J. Almahdawi, [3] Mohammed Ismael Hammed, [4]Hussein Burhan Mohammed

[1,2,3,4]Department of Mechanical Engineering, University of Diyala, Baqubah, Iraq

E-mail: 1m.sc.iman.m@engineering.uodiyala.edu.iq,

ABSTRACT

This study was conducted to determine the specific role of the effect of machining parameters spindle speed, feed rate and depth of cut on tool life during machining of AISI 316 under dry environment. The analysis was conducted under three different spindle speeds (300, 460 and 755 r.p.m.); feed rates (0.08, 0.1, 0.12mm/rev) and depths of cut (0.4, 0.8, 1.2mm). The used tools were coated carbide (WP9335) and HSS Co. The results showed that the spindle speed had the most significant effects on tool life than feed rate and depth of cut. The life of carbide tool when cutting the work materials was 473 sec, where the life of the HSS 65 sec, at spindle speed 300 rev/min, feed rate 0.08 rev/min and depth of cut 0.4mm, The shortest life of the two cutting tool materials (HSS, carbide) on the work material occurred at cutting speed (755 rpm), feed rate (0.12 mm/rev) and depth of cut (1.2 mm). The increment of spindle speed, feed rate and depth of cut values has great effect on the tool life.

Keywords - Cutting Parameters, Cutting Tools, Tool Life, Turning, Dry Machining

I. INTRODUCTION

Metal machining processes such as turning and cutting are widely used in engineering industries. Machining conditions (cutting speed, feed, and depth of cut) have represented the specific role in the efficient use of a machine tool and improving its tool life. Sunday Joshua Ojolo and Olugbenga Ogunkomaiya [1] presented an analysis of cutting tool life under different of cutting parameters (spindle speed, feed rate and depth of cut). Their results showed that the relationship between cutting parameters and tool life was most significant effects on spindle speed, than other parameters K.B. Ahsan, et al. [2] have found that as the cutting speed increases, the cutting tool life rapidly decrease due to high heat generation at the cutting zone, during α-β Ti-alloy machining the cutting zone, the chips the optimizinon of tool life of carbide inserts for turned parts using Taguchi's design of experiments approach. It was found from the results that the turning process parameters i.e. cutting speed, feed and depth of cut significantly affect the mean and variance of the tool life of the carbide inserts during turning En24 steel (0.4 % C). C.J. Raoa et al. [4] made analytical investigation of tool life during turning operation by determining optimal process parameters from MATLAB program. Their results indicated that the tool life decreases as the MRR and cutting speed optimization of cutting parameters for turning operations based on the Taguchi method. Their results showed that cutting parameters, cutting speed and feed rate tool life, while the change of the depth of cut within the selected range has an insignificant effect on tool life. Astakhov [6] studied the effect of the cutting feed, depth of cut, and workpiece (bore)

diameter on the tool wear rate. He found out that an increase in the feed rate leads to improved in tool life that's occur with optimal cutting temperature and cutting operation. In this work, the effect of machining parameters spindle speed, feed rate and depth of cut has been investigated on the tool life of carbide and HSS tool during machining of 316 stainless steel

II. MATERIALS

The experimental material used for this research work are two cutting tools, HSS cutting tool (12×12×150 HSS-Co) and carbide tool (wsp9335), as shown in figure (1). AISI 316 stainless steel was used as workpiece material with diameter 45mm×1200mm long as shown in figure (2)

Figure .1 Cutting tools, HSS-Co) and carbide tool(wsp9335)

Figure .2 Machining set up

III. EXPERIMENTAL PROCEDURE

Lathe machine F1-1000AG/ZJ with a spindle speed range from 70 to 1255 r.p.m.. was used for the79 machining trial. The experiment was done under dry machining environment. The following process parameters were used: Spindle speed of 300 r.p.m., 460 r.p.m. and 755rev/min, feed rate of 0.08mm/rev, 0.1mm/rev and 0.12 mm/rev, depth of cut of 0.4mm, 0.8mm and 1.2mm. The tool life is a measure of the amount of wear and the upper limit acceptable flank wear of 0.30 mm, as recommended by central machine tool institute, Figure .3 shows the relationship between the flank wear and tool life. Initial wear, steady wear, and severe wear periods are clearly observable from this figure.

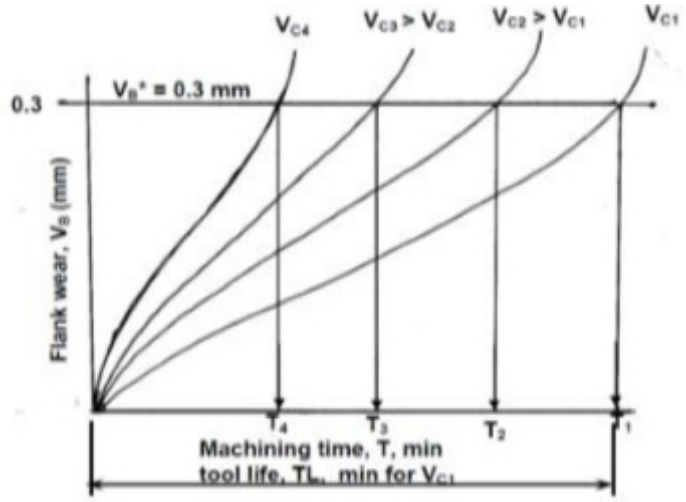

Figure 3: The relationship between the flank wear and tool life[7]

Figure .4: Lathe machine F1-1000AG/ZJ

IV. RESULTS AND DISCUSSION

The results of the experiments are presented in (Figures 3-16) and Table 1and 2

A- Carbide too

Figure (5) shows that the effect of spindle speeds of (300, 460, 755) r.p.m on tools life of the depths of cut (0.4, 0.8, and 1.2) mm at constant feed of 0.08 mm/rev. from Figure 2, it can be seen that the increase spindle speed from 300 r.p.m up to 755 r.p.m. at 0.4mm depth of cut resulted in decreasing tool life of carbide tool from 473sec to 237 sec i.e. approximately 50% reduction in tool life. Also, the same tendency is observed at depth of cut 0.8mm where the tool life reduces from 406 sec to 302 sec. Furthermore, the tool life reduces from 338 sec to 169 sec at depths of cut 1.2 mm. Figure (6) shows that the effect of spindle speeds of (300, 460, 755) r.p.m on tools life of the depths of cut (0.4, 0.8, 1.2) mm at constant feed of 0.1 mm/rev. it can be noticed that the tool life of carbide tool decrease from 445 sec to 223 sec with increasing spindle speed at depth of cut 0.4mm. While at depths of cut (0.8and 1.2) mm,

the tool life reduces from 382 sec to 191 sec and 318 sec to 159 sec respectively . Figure (7) reveals the effect of spindle speeds and depths of cut on tools life at constant value of feed rate (0.12 mm/rev). it can be observed from Figure 4 that the increase in the spindle speed at 0.4 mm value of depth of cut causes decreasing the tool life of carbide tool from 432 sec to 210 sec i.e. 51% reduction in tool life. While at depths of cut (0.8 mm), the tool life reduces from 370 sec to 180 sec and at depth of cut 1.2 mm, the tool life reduces from 309 sec to 150 sec. This is due to its high wear resistance. It can be seen that better tool life is obtained with an arrangement of spindle speed 300) r.p.m, feed 0.08 mm/rev, and depth of cut 0.4 and this results agreed with Tugrul and Karpat.[8]. From the results it can be concluded that the better tool life is obtained at lowest value of feed rate and lowest value of cutting speed. Figure 5 shows the effect of the feed rates at (0.08, 0.1, 0.12) mm/rev values on the tool life under different spindle speeds (300, 460, 755) r.p.m with constant value of depth of cut at 0.4mm. it can be noticed that as the feed rate increases from 0.08mm/rev up to 0.12mm/rev with 300 r.p.m spindle speed, the tool life decreases from 473 sec to 433 sec. While the tool life decrease from 393 sec to 346 sec at spindle speed of 460 rev/min with the different value of feed rate. The same trend of tool life was observed at constant value of spindle speed (755 r.p.m) where the tool life reduces from 237 sec to 203 sec. It is clear from the results above that the value of feed rate at 0.12 mm/rev results in shorter tool life in all cases. It can be concluded from the results that the increasing in the feed rate leads to decreases in the tool life when cutting speed and depth of cut are both constant and this results agree with previous researches [9].

N(rpm)	F(mm/rev)	Tool life (sec.) of carbide tool		
		d(mm) 0.4	d(mm) 0.8	d(mm) 1.2
300	0.08	473	406	338
460	0.08	393	337	281
755	0.08	237	203	169
300	0.1	445	382	318
460	0.1	371	318	265
755	0.1	223	191	159
300	0.12	432	370	309
460	0.12	354	296	247
755	0.12	210	180	150

Table:1 Cutting Parameters with tool life of carbide tool

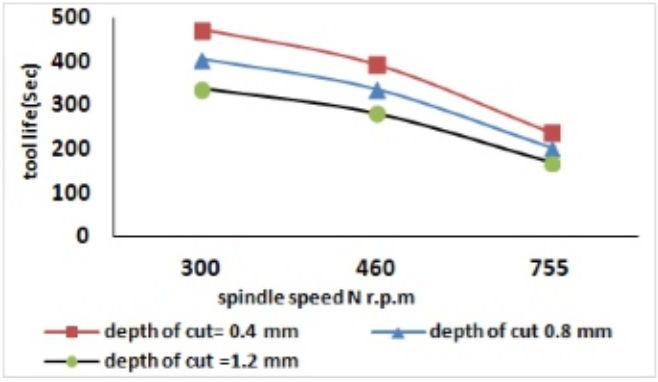

Fig 5: Effect of spindle speed on life of tools under different depth of cut a constant Feeds rate 0.08mm /rev for carbide tool

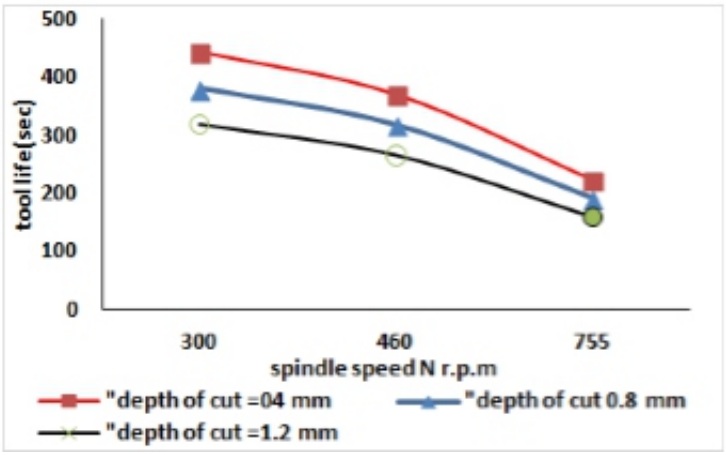

Figure 6: Effect of spindle speed on life of tools under different depth of cut at constant Feeds rate 0.1 mm /rev for carbide tool

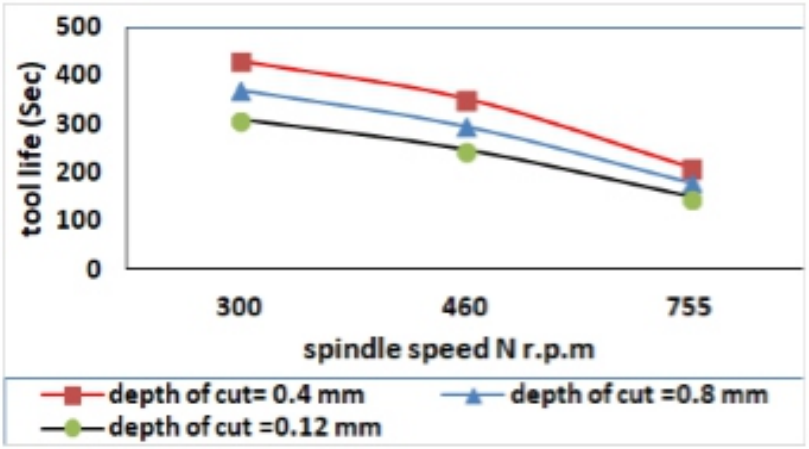

Figure 7: Effect of spindle speed on life of tools under different depth of cut at constant Feeds rate 0.12mm /rev for carbide tool

It was observed from Figure (8) that as the feed rate increased from 0.08mm/rev up to 0.12mm/rev with 300) r.p.m value of spindle speed, the tool life of carbide tool decreased from 406s sec to 350 sec. It can be seen the same behavior of tool life when the spindle speed is 460 r.p.m. Also, the same trend was observed at constant spindle speed of 755rev/min, the tool life of carbide tool reduced from 250 sec to 160 sec. Figure (9) shows the effect of the feed rates of (0.08, 0.1, 0.12) mm/rev on tools life for carbide tool under different spindle speeds (300, 460, 755) r.p.m and at constant depth of cut 0.8mm. Figure (10) shows the effect of the feed rates of (0.08, 0.1, 0.12) mm/rev on tools life for carbide tool under different spindle speeds (300, 460, 755) r.p.m and at constant depth of cut 1.2 mm. As the feed rate increased from 0.08mm/rev up to 0.12mm/rev, it was observed that at 300) r.p.m spindle speed, the tool life of carbide tool decreased from 338 sec to 309 sec. At a spindle speed of 460 rev/min, there was a decrease in the tool life from 281 sec to 247 sec .The same trend was observed at constant spindle speed of 755 r.p.m where the tool life of tungsten carbide reduced from 169 sec to 150 sec.

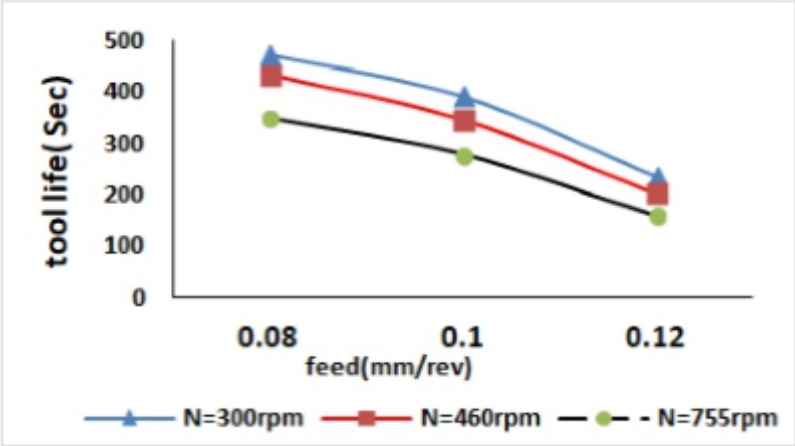

Figure.8: Effect of Feeds rate on life of tools under different Spindle speed at constant depth of cut 0.4.mm for carbide tool

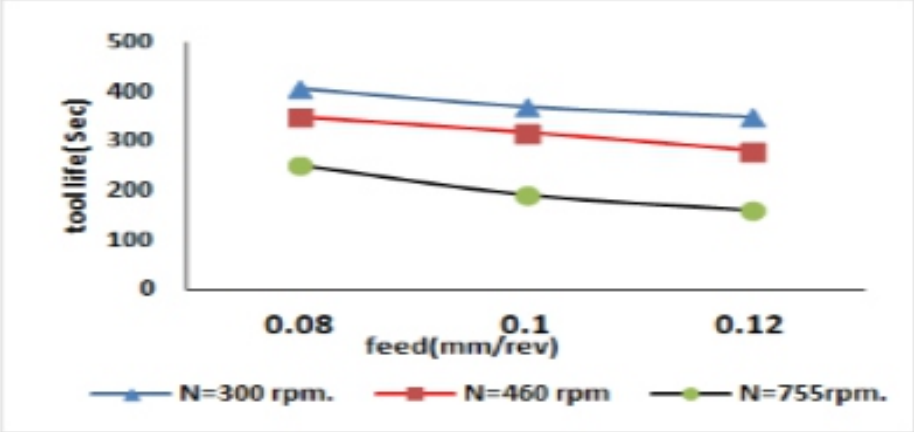

Figure.9: Effect of feeds rate on life of tools under different Spindle speed at constant depth of cut 0.8 mm for carbide tool

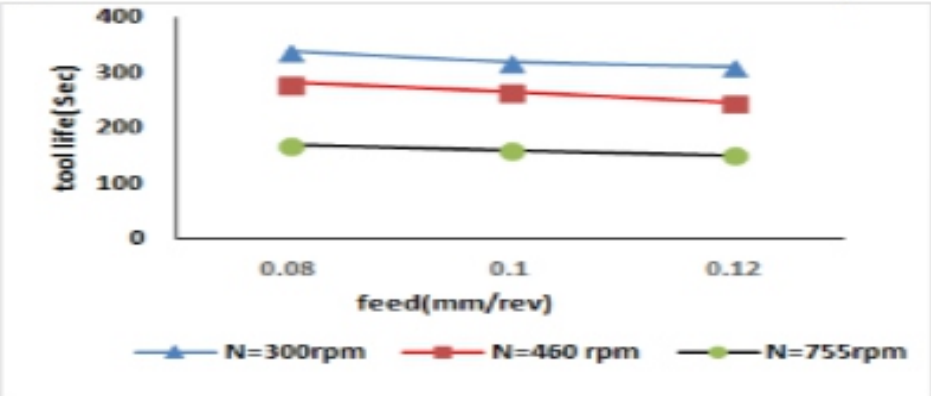

Figure 10: Effect of feeds rate on life of tools under different Spindle Speed at constant depth of cut 1.2.mm for carbide tool

B- HSS Tool.

Figure (11) shows that the effect of spindle speeds of (300, 460, 755) r.p.m on tools life of the depths of cut(0.4,0.8,1.2)mm at constant feed of 0.08 mm/rev. as the spindle speed increased from 300rev/min up

to 755 r.p.m at 0.4mm depth of cut, the tool life of HSS tool decreases from 65 sec to 38 sec, also the same tendency was observed at depth of cut 0.8mm where the tool life reduces from 37 sec to 27 sec and at depths of cut 1.2 mm the tool life reduced from 25 sec to 10 sec. This due to the fact that the contact length of the cutting edge with the work-piece increases with increase the depth of cut. Thus wear occurs deeper along the cutting edge and causes reducing in the tool life of HSS [10]. Figure (12) shows that the effect of spindle speeds of (300, 460, 755) r.p.m on tools life of the depths of cut (0.4,0.8,1.2) mm at constant feed of 0.1 mm/rev, as the spindle speed increased from 300rev/min up to 755 r.p.m. at 0.4mm depth of cut, the tool life of HSS tool decreases from60 sec to 30 sec, at depths of cut 0.8 mm the tool life reduces from 35 sec to 23 sec and depth of cut 1.2 mm the tool life reduces from 22 sec to 8 sec, At constant feed of 0.12 mm/rev figure (13) shows that the effect of spindle speeds of (300, 460, 755) r.p.m on tools life of the depths of cut (0.4,0.8,1.2)mm, when the spindle speed increased from 300) r.p.m up to 755 r.p.m, the tool life of HSS tool decreases dramatically from50 sec to28 sec at 0.4 mm depth of cut , at depths of cut 0.8 mm the tool life reduced from 30 sec to20 sec and depth of cut 1.2 mm, the tool life reduced from 20 sec to 7 sec. Increase in depth of cut cause more materials removal from work piece, which means more energy will be required and this will cause an increase in the cutting force and this decreases tool life. In addition, the increase in the cutting feed leads to a decrease in the tool life, according to the change in the temperature, that's leads to shorter tool life. However if the cutting speed is low, the cutting temperature will be lower than the optimal cutting temperature, leading to longer tool life. This results agree with Viktor P. Astakhov [6]. At the value of spindle speed of 755rev/min and feed rate up to 0.12mm/rev, the tool life of HSS decreases from 14 sec to 7 sec .This decreasing in tool life occurs due to the wear on the cutting edge. That's might be due to increase in feed rate that causes larger contact area between cutting tool and work-piece, the bigger interface, resulted in more friction that caused more heat generated and consequently shorten the tool.

N(rpm)	F(mm/rev)	Tool life (sec.) of HSS tool		
		d(mm) 0.4	d(mm) 0.8	d(mm) 1.2
300	0.08	65	37	25
460	0.08	55	35	22
755	0.08	45	30	20
300	0.1	55	33	20
460	0.1	50	31	18
755	0.1	38	27	16
300	0.12	50	27	14
460	0.12	40	23	10
755	0.12	28	20	7

Table:2 cutting parameters with tool life of HSS tool

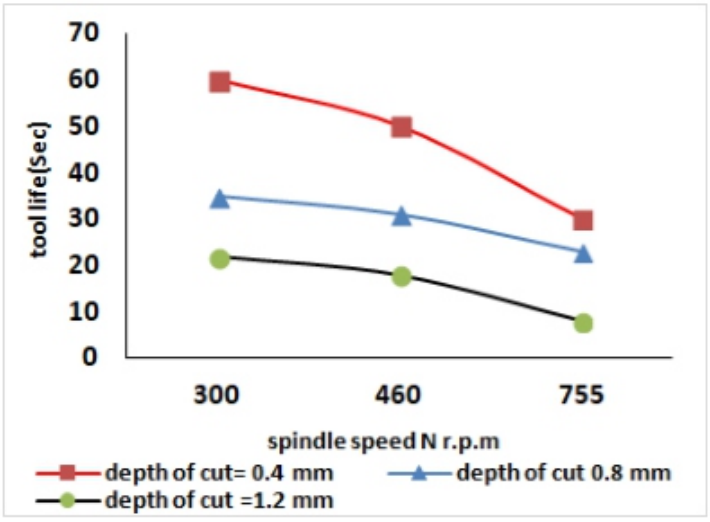

Figure 11: Effect of spindle speed on life of tools under different depth of cut at constant Feeds rate 0.08 mm /rev for carbide tool for HSS

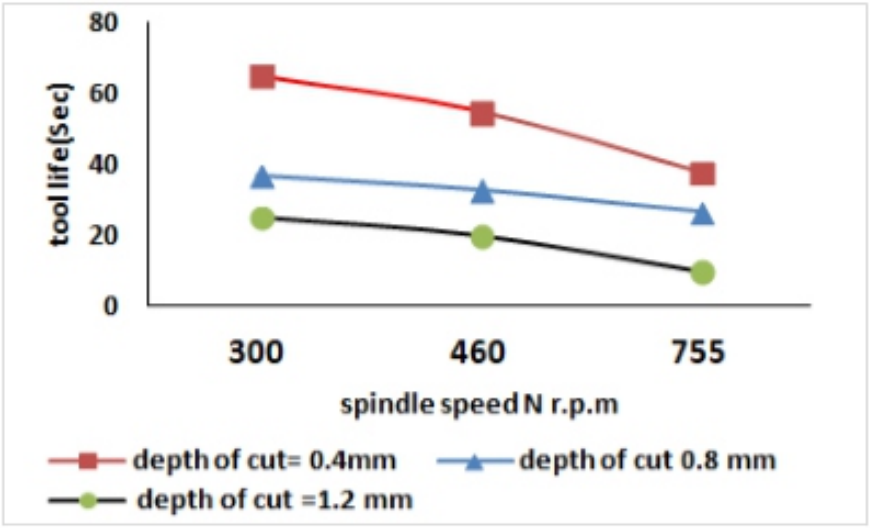

Figure 12: Effect of spindle speed on life of tools under different depth of cut at constant Feeds rate 0.1 mm /rev for carbide tool for HSS

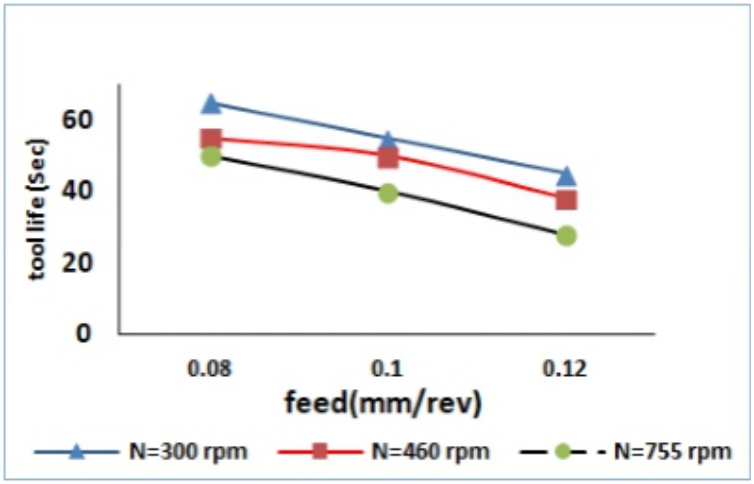

Figure 13: Effect of spindle speed on life of tools under different depth of cut at constant Feeds rate 1.2 mm /rev for carbide tool for HSS

Figure (14) shows the effect of the feed rates of (0.08, 0.1, 0.12) mm/rev on tools life for carbide tool under different spindle speeds (300, 460, 755) r.p.m and at constant depth of cut 0.4mm. As the feed rate increased from 0.08mm/rev up to 0.12mm/rev, it was observed that at 300 rev/min spindle speed, the tool life of HSS tool decreased from 65 sec to 45 sec showing 30% reduction in the tool life. At a spindle speed of 460 r.p.m there was a decrease in the tool life from 55 sec to 38 sec. The same trend was observed at constant spindle speed of 755 r.p.m, the tool life of HSS reduces from 50 sec to 28 sec. At these conditions, the effect of feed at 0.12 mm/rev is clear ontool life giving shorter tool life in all cases and this agrees with previous study [9]. Figure (15) represents the effect of the feed rates of (0.08, 0.1, 0.12) mm/rev on tools life for HSS tool under different spindle speeds (300, 460, 755) r.p.m. and at constant depth of cut 0.8mm. It was observed that as the feed rate increases from 0.08mm/rev up to 0.12mm/rev, at 300 rev/min spindle speed, the tool life of HSS tool decreases from 37 sec to 30 sec. At a spindle speed of 460) r.p.m, there was a decrease in the tool life from 33 sec to 27 sec .The same trend was observed at constant spindle speed of 755) r.p.m, the tool life of HSS reduced from 27 sec to 20 sec. Figure (16) reveals the effect of the feed rates of (0.08, 0.1, 0.12) mm/rev on tools life for HSS tool under different spindle speeds (300, 460, 755)) r.p.m, and at constant depth of cut 1.2 mm. As the feed rate increases from 0.08mm/rev up to 0.12mm/rev, it was observed that at 300 rev/min spindle speed, the tool life of carbide tool decreased from 25 sec to 20 sec. At a spindle speed of 460 r.p.m, there was a decrease in the tool life from 20 sec to 16 sec. The same trend was observed at constant spindle speed of 755 r.p.m. the increasing in the depth of cut up to 1.2 mm causes the compressive stress on the cutting edge which causes in rapid fracture of the tool so resulting in a decrease in the tool life from 14 sec to 7 sec. This fact can be attributed to increase depth of cut reduces tool life but essentially increases the amount of the removed material by the tool. At these conditions, the effect of depth of cut at 1.2 mm was evident on tool life giving shorter in tool life for all cases. cases.

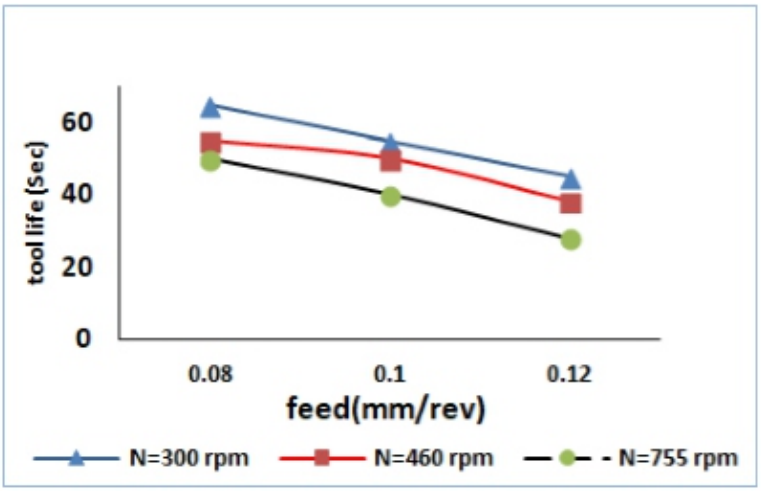

Figure 14: Effect of Feeds rate on life of tools under different Spindle speed at constant depth of cut 0.4.mm for HSS tool

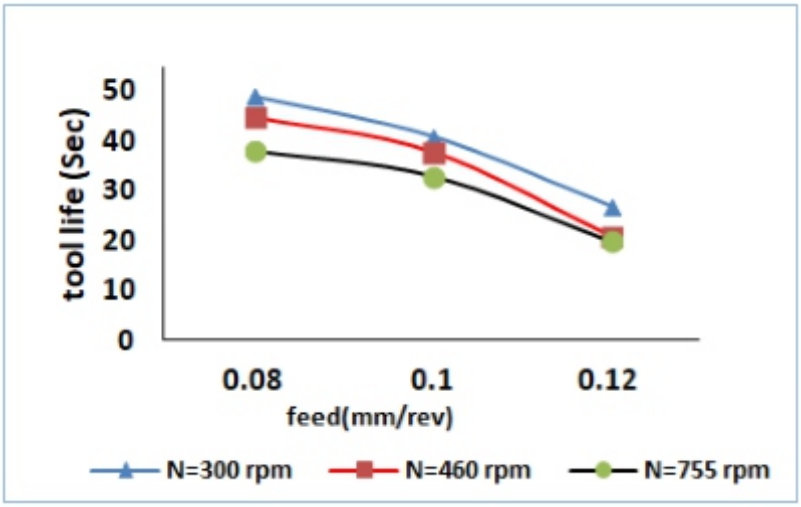

Figure. 15: Effect of feeds rate on life of tools under different Spindle speed at constant depth of cut 0.8 mm for HSS tool

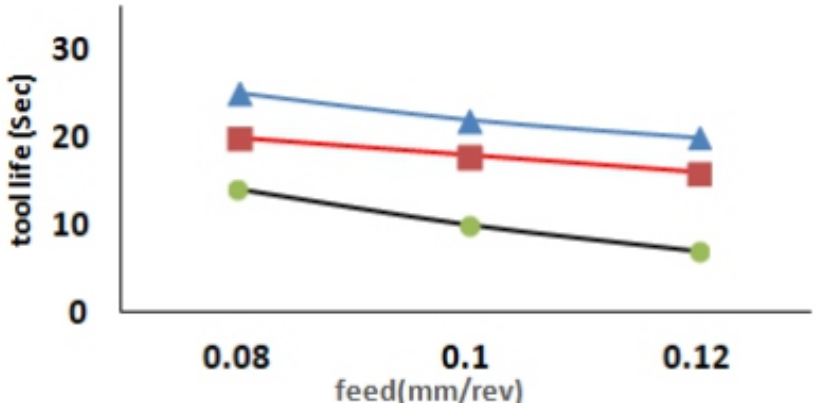

Figure .16: Effect of feeds rate on life of tools under different Spindle speed at constant depth of cut 1.2 .mm for HSS tool

V. CONCLUSION

The following conclusions can be drawn from this study:

- From the cutting parameters which affect the machining process, spindle speed has a great effectiveness on tool life and more efficiency than the feed rate and depth of cut
- The feed rate at (0.08 mm/rev) was evident effect on tool life giving shorter tool life in all cases.
- Carbide tool has the longest tool life than the HSS tool.
- The lower cutting speeds should be selected in arrangement with suitable feed rate that's leads to the conclusion that for improved tool life.

ACKNOWLEDGMENTS

The author wish to acknowledge to the Department of mechanical Engineering on university of Diyala for making available their facilities to carry out the experiments.

REFERENCES

[1] S.J.Ojolo " A study of effects of machining parameters on tool life", International Journal of Materials Science and Applications. Vol. 3 pp. 183-199. 2014,

[2] K.B. Ahsan, A.M. Mazid, R.E. Clegg, G.K.H. Pang," Study on carbide cutting tool life using various cutting speeds for α-β Ti-alloy machining", Journal of Materials and manufacturing engineering. Vol. 55, pp. 600-606. 2012,

[3] H. Singh, "Optimizing Tool Life of Carbide Inserts for Turned Parts using Taguchi's Design of Experiments Approach". Proceedings of the International Multi Conference of Engineers and Computer Scientists. March, Vol II, pp. 978-988,2008

[4] C.J. Raoa* D. Sreeamulua A.T. Mathewb Procedia Engineering (2014) ,pp. 241-250. Vol. 55, No. 2,

[5] W.H. Yang and Y.S. Tarng, "Design optimization of cutting parameters for turning operations based on the Taguchi method," Journal of Materials Processing Technology, vol.34, pp. 122-129, 1998.

[6] V. Astakhov, "Effects of the cutting feed, depth of cut, and workpiece (bore) diameter on the tool wear rate," International Journal of Advanced Manufacturing Technology, 2006.

[7] Central Machine Tool Institute Bangalore, India, Tata McGraw-Hill Pub., 1985 Machine Tool Design Handbook

[8] Tugrul and Y. Karpat, "Multi-objective optimization for turning processes using neural network modeling and dynamic neighborhood particle swarm optimization," International Journal Advance Manufacturing Technology, pp. 234-247, 2007.

[9] F.E. Gorczyca, "Application of metal cutting theory", New York: Industrial Press, 1987.

[10] S.R. Das, R.P. Nayak and D. Dhupal, "Optimization of cutting parameter on tool wear and workpiece surface temperature in turning of AISI D2 steel,"International Journal of Lean Thinking, vol. 3, no 2, pp. 140-156,2012.

Monitoring of Production Process at Production of Components in Automotive Industry

[1] Jozef Dobransky, [2] Jozef Svetlik, [3] Zigmund Dobos

[1,3]Technical University of Košice, Faculty of Manufacturing Technologies with a seat in Prešov, Štúrova 31, Prešov, Slovak Republic,

[2]Technical University of Košice, Faculty of Mechanical Engineering, Letná 9, Košice, Slovak Republic,

E-mail: [1]jozef.dobransky@tuke.sk, [2]jozef.svetlik@tuke.sk, [3]doboszig@gmail.com

A B S T R A C T

This paper deals with assessment of capability of production process of manufacturing of components in automotive industry by injection molding technology. Assessment of quality of production process in automotive industry is very important. Components used in this industry must be of high quality. According to the analysis of production process capability, the process is well set. Products made by this process have high quality.

Keywords - Automotive Industry, Capability, Production Process, Quality.

I. INTRODUCTION

For quality improvement, it is necessary to know and use appropriate tools, such as methods and models of statistical quality management. Effective program of quality improvement leads to keeping, or improving product's position on the market, decreasing of manufacturing expenses a higher productivity. Currently, it is difficult to keep high quality [1].

Fast development of technology complicates keeping the quality at an appropriate level. Nowadays, quality management is not carried out only at the end of production process for elimination of defective products. The process of quality management concerns not only the product, but also the production processes. Quality management is the way to increase clients' satisfaction and company's market share [2].

Quality management is defined as a summary of all tools needed for achieving quality standards. In other words, quality management is planning and realization of tools for production of a product, which will be highly useful and will satisfy client's needs [3].

Quality management which is limited to technical aspects is not complex. Complex management requires involvement of other departments, such as company's management and sales. Quality of product includes all its attributes, not only its technical properties [4].

This is total quality management. According to Feigenbaum's definition, quality management concerns all departments and levels, while everything is oriented on common goal, i.e. on providing a high quality product for a reasonable price [5].

Statistical regulation of the SPC processes is the method of the quality control applying the statistical methods. It is applied to monitor and control the process. The regulation consists of two phases: the first one refers to initial adjustment of specifications of the selected process; the second one represents the case of common process utilization in the production. In comparison to other methods of the quality control the advantage of application of the SPC method rests in preference of timely detection and prevention of occurrence of problematic situations prior to correction of already occurred situations [6].

II. DESCRIPTION OF THE EXPERIMENT

The aim of the experiment was to perform an analysis of capability of production process. Plastic component used in automotive industry for production of automobiles was utilized for this analysis.

A. Analysis of Capability of Production Process

The aim of capability process index is to simply explain the relation between Target Value T, Specification Limits LSL, USL, and the real process expressed by Medium Value μ, and Standard Deviation σ of measured values of chosen attribute of quality process. Target Value T is required medium value of quality attribute, which needs to be attained as closely as possible. Lower and Upper Specification Limit LSL, USL are limits set for a particular quality attribute considering required variability, with the aim to ensure required functionality of the product, semi-finished product and etc.

The data analysis of the process capability can be applied especially in the following spheres:

- prognosis of the process measure during its progress within the scope of tolerance limits,
- selection or modification of the process,
- determination of interval width in statistical regulation of the process,
- specification of the requirements for new equipment performance,
- selection of suppliers,
- planning of succession of production processes in case the interactive influence of the processes upon the tolerances exist,
- reduction of variability in the process.

B. Plastic Product Used for Analysis

The analyzed plastic product used for statistical regulation of production processes was a light cover in automobile produced by injection molding technology. Figure 1 shows correct measurement of a component together with evaluated dimensional characteristics.

In the serial production process of this plastic product, verification is performed in the following steps:

- Input material verification
- Verification of design of the plastic product
- Verification of dimensions
- Verification of processes

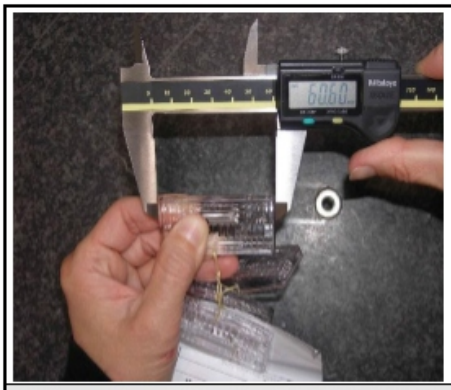

Measured values					
1.	Upper limit	60.72	2.	Upper limit	26.54
	Total length	60.62		Total width	26.44
	Lower limit	60.52		Lower limit	26.34

Fig. 1 Graphic description of measurement and measured dimensional characteristics

III. EVALUATION

Analyzed component is produced in double cavity mold. Plastic products were therefore analyzed individually. Cavity 1 Capability Indices in cavity 1 had the following values: total length Cp = 2.058, Cpk = 2.012 (Fig. 2) and total width Cp = 3.837, Cpk = 3.829 (Fig. 3). Based on these values, we can state that the process is capable and well centered.

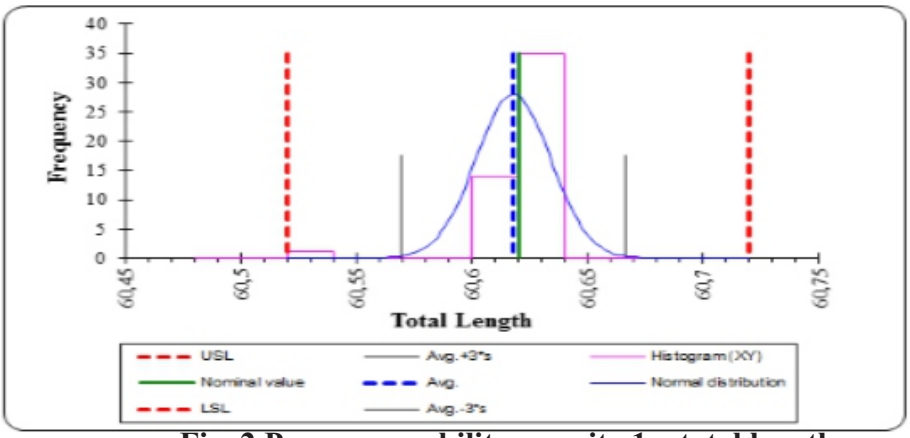

Fig. 2 Process capability – cavity 1 – total length

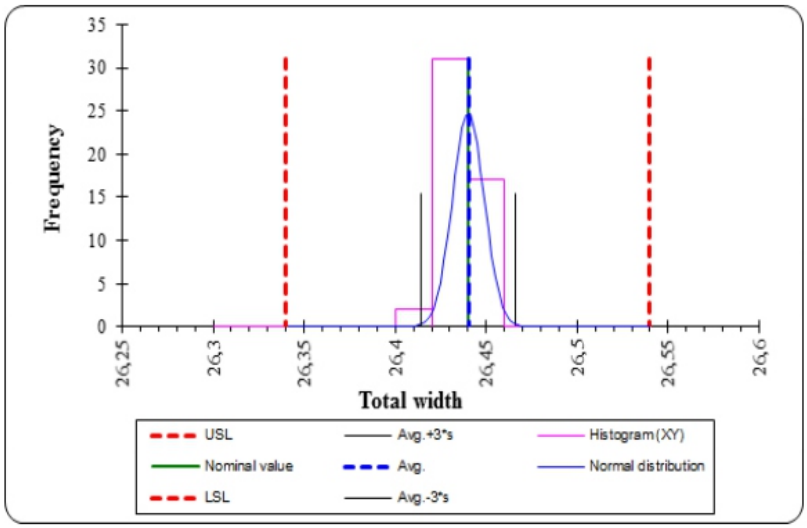

Fig. 3 Process capability – cavity 1 – total width

Cavity 2

As we can see on these graphs, plastic products from cavity no.2 are also of high quality and based on capability indices values we can conclude the process is capable and well centred. Indices values: total length Cp = 2.298, Cpk = 2.123 (Fig. 4) and total width is Cp = 3.689, Cpk = 3.542 (Fig. 5).

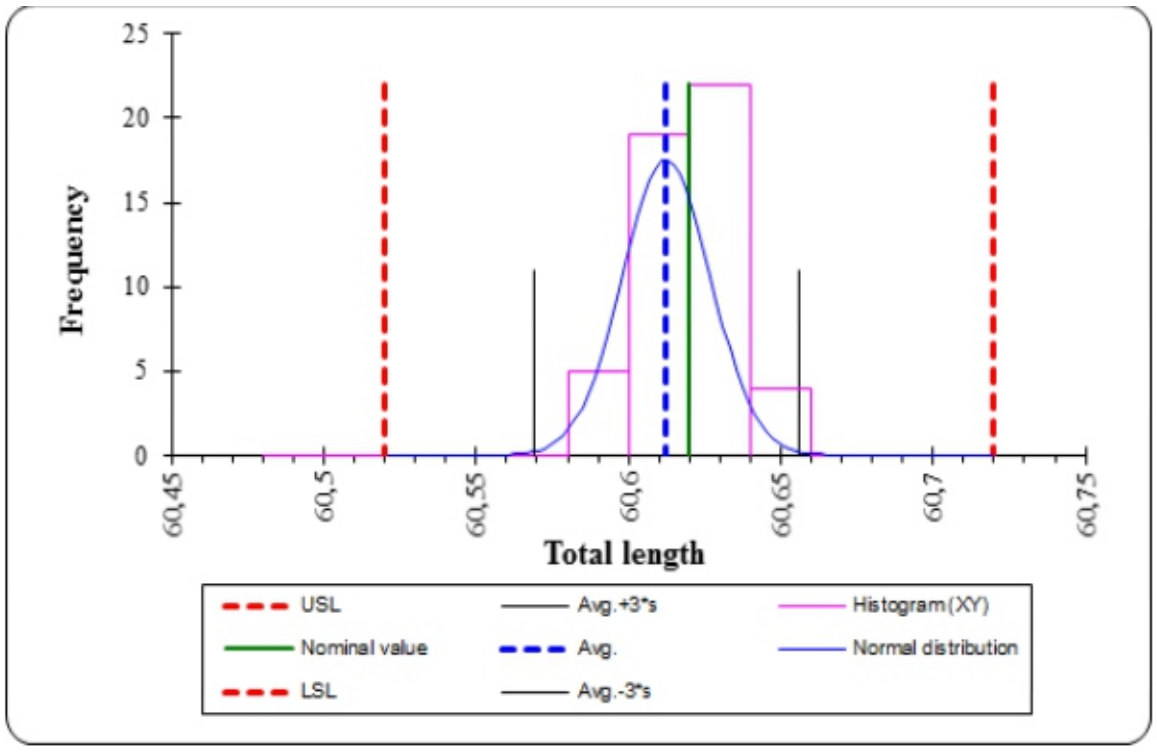

Fig. 4 Process capability – cavity 2 – total length

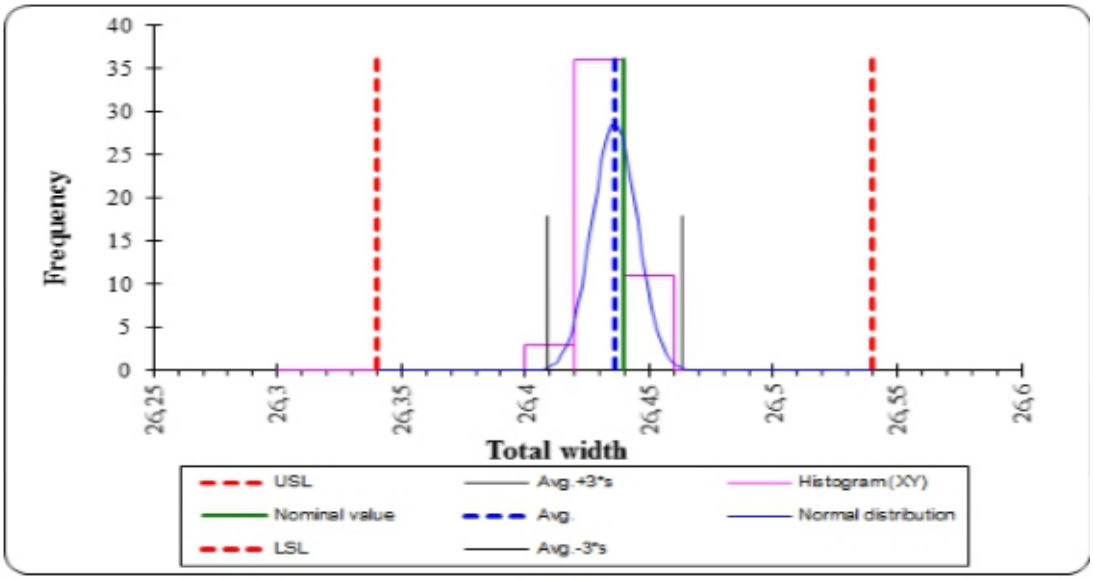

Fig. 5 Process capability – cavity 2 – total width

IV. CONCLUSION

Every process shows a certain variability. The process is always affected by a number of influences that cause differences in products. The aim of statistical methods is to study theses influences and to create conditions that make variability of the process stable. Before collection of data for calculation of capability indices, it is necessary to check the system of measurement of a chosen quality attribute, in order to get results that correctly represent the real process capability. For the analysis of the system of measurement a method of an average and a range was used. This method is used for evaluation of repeatability and reproducibility of measurement. It was applied by three different inspectors performing measurements of total length and width on the products from two different cavities of injection mold, since it was a double cavity injection mold. Capability of production process was carried out after the analysis of measurement process. Capability of the process was evaluated based on capability indices. The quality of the production process was at high level which was supported by capability indices.

ACKNOWLEDGMENT

This paper has been elaborated in the framework of the project KEGA no. 006TUKE-4/2017 Innovation of Laboratory quality control of components for the automotive and allied industries within the framework of the integration of advanced cognitive operations into education and project APVV-15-0149 Research of new measuring methods of machine condition.

REFERENCES

[1] J. Dobránsky, A. Panda, and D. Manduľák, "Quality monitoring in production of the parts in automotive industry," IEEE Trans. on Neural Networks, Lüdenscheid : RAM - Verlag, 2015.

[2] R. Kreheľ, and M. Pollák, "The contactless measuring of the dimensional attrition of the cutting tool and roughness of machined surface," In: International Journal of Advanced Manufacturing Technology. Vol. 86, no. 1-4 (2016), p. 437-449, 2016.

[3] J. Dobránsky, J. Ružbarský, D. Manduľák, and E. Vojnová, "Monitoring of the Production Process in Mass Production of Dimensionally Accurate Products," TEM Journal, vol. 5, no. 2, pp. 175-179, 2016.

[4] Ľ. Straka, and S. Hašová, "Assessing the influence of technological parameters on the surface quality of steel MS1 after WEDM," In: MM Science Journal. Vol. 2016, p. 1194-1200, 2016.

[5] J. Dobránsky, F. Botko and E. Vojnová, "Monitoring of production quality for plastic component," In: MM Science Journal. Vol. 2016, p. 1073-1076, 2016.

[6] J. Dobránsky, E. Ragan and N. Daneshjo, "Determination of technological parameters limit values on planned experiment, proposal for following products from thermoplastics qualitative parameters," In: Engineering Review. Vol. 29, No. 2 p. 45-51, 209.

Instructions for Authors

Essentials for Publishing in this Journal

1 Submitted articles should not have been previously published or be currently under consideration for publication elsewhere.

2 Conference papers may only be submitted if the paper has been completely re-written (taken to mean more than 50%) and the author has cleared any necessary permission with the copyright owner if it has been previously copyrighted.

3 All our articles are refereed through a double-blind process.

4 All authors must declare they have read and agreed to the content of the submitted article and must sign a declaration correspond to the originality of the article.

Submission Process

All articles for this journal must be submitted using our online submissions system. http://enrichedpub.com/ . Please use the Submit Your Article link in the Author Service area.

Manuscript Guidelines

The instructions to authors about the article preparation for publication in the Manuscripts are submitted online, through the e-Ur (Electronic editing) system, developed by **Enriched Publications Pvt. Ltd**. The article should contain the abstract with keywords, introduction, body, conclusion, references and the summary in English language (without heading and subheading enumeration). The article length should not exceed 16 pages of A4 paper format.

Title

The title should be informative. It is in both Journal's and author's best interest to use terms suitable. For indexing and word search. If there are no such terms in the title, the author is strongly advised to add a subtitle. The title should be given in English as well. The titles precede the abstract and the summary in an appropriate language.

Letterhead Title

The letterhead title is given at a top of each page for easier identification of article copies in an Electronic form in particular. It contains the author's surname and first name initial .article title, journal title and collation (year, volume, and issue, first and last page). The journal and article titles can be given in a shortened form.

Author's Name

Full name(s) of author(s) should be used. It is advisable to give the middle initial. Names are given in their original form.

Contact Details

The postal address or the e-mail address of the author (usually of the first one if there are more Authors) is given in the footnote at the bottom of the first page.

Type of Articles

Classification of articles is a duty of the editorial staff and is of special importance. Referees and the members of the editorial staff, or section editors, can propose a category, but the editor-in-chief has the sole responsibility for their classification. Journal articles are classified as follows:

Scientific articles:

1. Original scientific paper (giving the previously unpublished results of the author's own research based on management methods).
2. Survey paper (giving an original, detailed and critical view of a research problem or an area to which the author has made a contribution visible through his self-citation);
3. Short or preliminary communication (original management paper of full format but of a smaller extent or of a preliminary character);
4. Scientific critique or forum (discussion on a particular scientific topic, based exclusively on management argumentation) and commentaries. Exceptionally, in particular areas, a scientific paper in the Journal can be in a form of a monograph or a critical edition of scientific data (historical, archival, lexicographic, bibliographic, data survey, etc.) which were unknown or hardly accessible for scientific research.

Professional articles:

1. Professional paper (contribution offering experience useful for improvement of professional practice but not necessarily based on scientific methods);
2. Informative contribution (editorial, commentary, etc.);
3. Review (of a book, software, case study, scientific event, etc.)

Language

The article should be in English. The grammar and style of the article should be of good quality. The systematized text should be without abbreviations (except standard ones). All measurements must be in SI units. The sequence of formulae is denoted in Arabic numerals in parentheses on the right-hand side.

Abstract and Summary

An abstract is a concise informative presentation of the article content for fast and accurate Evaluation of its relevance. It is both in the Editorial Office's and the author's best interest for an abstract to contain terms often used for indexing and article search. The abstract describes the purpose of the study and the methods, outlines the findings and state the conclusions. A 100- to 250- Word abstract should be placed between the title and the keywords with the body text to follow. Besides an abstract are advised to have a summary in English, at the end of the article, after the Reference list. The summary should be structured and long up to 1/10 of the article length (it is more extensive than the abstract).

Keywords

Keywords are terms or phrases showing adequately the article content for indexing and search purposes. They should be allocated heaving in mind widely accepted international sources (index, dictionary or thesaurus), such as the Web of Science keyword list for science in general. The higher their usage frequency is the better. Up to 10 keywords immediately follow the abstract and the summary, in respective languages.

Acknowledgements

The name and the number of the project or programmed within which the article was realized is given in a separate note at the bottom of the first page together with the name of the institution which financially supported the project or programmed.

Tables and Illustrations

All the captions should be in the original language as well as in English, together with the texts in illustrations if possible. Tables are typed in the same style as the text and are denoted by numerals at the top. Photographs and drawings, placed appropriately in the text, should be clear, precise and suitable for reproduction. Drawings should be created in Word or Corel.

Citation in the Text

Citation in the text must be uniform. When citing references in the text, use the reference number set in square brackets from the Reference list at the end of the article.

Footnotes

Footnotes are given at the bottom of the page with the text they refer to. They can contain less relevant details, additional explanations or used sources (e.g. scientific material, manuals). They cannot replace the cited literature.

The article should be accompanied with a cover letter with the information about the author(s): surname, middle initial, first name, and citizen personal number, rank, title, e-mail address, and affiliation address, home address including municipality, phone number in the office and at home (or a mobile phone number). The cover letter should state the type of the article and tell which illustrations are original and which are not.

Address of the Editorial Office:

Enriched Publications Pvt. Ltd.
S-9,IInd FLOOR, MLU POCKET,
MANISH ABHINAV PLAZA-II, ABOVE FEDERAL BANK,
PLOT NO-5, SECTOR -5, DWARKA, NEW DELHI, INDIA-110075,
PHONE: - + (91)-(11)-45525005

Notes: